ChemPubSoc Europe

DOI: 10.1002/chem.201504030

CHEMISTRY A European Journal Full Paper

N-Heterocyclic Carbenes |*Hot Paper*|

Homo- and Heterodinuclear Ir and Rh Imine-functionalized Protic NHC Complexes: Synthetic, Structural Studies, and Tautomerization/Metallotropism Insights**

Fan He,[a] Marcel Wesolek,[a] Andreas A. Danopoulos,*[a, b] and Pierre Braunstein*[a]

Dedicated to Prof. Dr. Herbert W. Roesky on the occasion of his 80th birthday

Abstract: The influence of the potentially chelating imino group of imine-functionalized Ir and Rh imidazole complexes on the formation of functionalized protic N-heterocyclic carbene (pNHC) complexes by tautomerization/metallotropism sequences was investigated. Chloride abstraction in [Ir(cod)Cl{$C_3H_3N_2$(DippN=CMe)-κN3}] (**1a**) (cod = 1,5-cyclooctadiene, Dipp = 2,6-diisopropylphenyl) with $TlPF_6$ gave [Ir(cod){$C_3H_3N_2$(DippN=CMe)-κ^2(C2,N_{imine})}]$^+$[PF_6]$^-$ (**3a**$^+$[PF_6]$^-$). Plausible mechanisms for the tautomerization of complex **1a** to **3a**$^+$[PF_6]$^-$ involving C2–H bond activation either in **1a** or in [Ir(cod){$C_3H_3N_2$(DippN=CMe)-κN3}$_2$]$^+$[PF_6]$^-$ (**6a**$^+$[PF_6]$^-$) were postulated. Addition of PR_3 to complex **3a**$^+$[PF_6]$^-$ afforded the eighteen-valence-electron complexes [Ir(cod)(PR_3){$C_3H_3N_2$(DippN=CMe)-κ^2(C2,N_{imine})}]$^+$[PF_6]$^-$ (**7a**$^+$[PF_6]$^-$ (R = Ph) and **7b**$^+$[PF_6]$^-$ (R = Me)). In contrast to Ir, chloride abstraction from [Rh(cod)Cl{$C_3H_3N_2$(DippN=CMe)-κN3}] (**1b**) at room temperature afforded [Rh(cod){$C_3H_3N_2$(DippN=CMe)-κN3}$_2$]$^+$[PF_6]$^-$ (**6b**$^+$[PF_6]$^-$) and [Rh(cod){$C_3H_3N_2$(DippN=CMe)-κ^2(C2,N_{imine})}]$^+$[PF_6]$^-$ (**3b**$^+$[PF_6]$^-$) (minor); the reaction yielded exclusively the latter product in toluene at 110 °C. Double metallation of the azole ring (at both the C2 and the N3 atom) was also achieved: [Ir_2(cod)$_2$Cl{μ-$C_3H_2N_2$(DippN=CMe)-κ^2(C2,N_{imine}),κN3}] (**10**) and the heterodinuclear complex [IrRh(cod)$_2$Cl{μ-$C_3H_2N_2$(DippN=CMe)-κ^2(C2,N_{imine}),κN3}] (**12**) were fully characterized. The structures of complexes **1b**, **3b**$^+$[PF_6]$^-$, **6a**$^+$[PF_6]$^-$, **7a**$^+$[PF_6]$^-$, [Ir(cod){C_3HN_2(DippN=CMe)(DippN=CH)(Me)-κ^2(N3,N_{imine})}]$^+$[PF_6]$^-$ (**9**$^+$[PF_6]$^-$), **10**·Et_2O·toluene, [Ir_2(CO)$_4$Cl{μ-$C_3H_2N_2$(DippN=CMe)-κ^2(C2,N_{imine}),-κN3}] (**11**), and **12**·2THF were determined by X-ray diffraction.

Introduction

Since the isolation of N-heterocyclic carbenes (NHCs),[1] their study and complexation chemistry have generated a rapidly increasing interest.[2] In most of their metal complexes, both N atoms carry substituents R (R = R′ or R ≠ R′ in Scheme 1 A) that allow fine-tuning of the steric and electronic properties of the NHC ligands. Protic NHC (pNHC) metal complexes (Scheme 1 B) are less common. The N–H moiety can further be a reactive site, for example, with bases or hydrogen-bond acceptors, the latter being relevant to substrate recognition in homogeneous catalysis.[3]

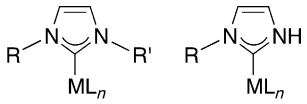

A **B**

Scheme 1. Different structures of substituted NHC metal complexes

pNHCs cannot be generally obtained by simple deprotonation of the corresponding imidazolium salts owing to the presence of sites with acidity (i.e., N–H group) comparable to the C2–H group on the heterocycle; furthermore, the free pNHCs are not stable and tend to isomerize to the corresponding imidazoles.[4] This has motivated the development of various methods to access pNHC metal complexes, which have been recently summarized and reviewed.[3b,c,5] The first transition-metal complex bearing 1*H*-imidazol-2-ylidene (R = H in Scheme 1 B) was obtained by the acid-catalyzed rearrangement of a Ru^{II}–imidazole to a Ru^{II}–pNHC system (Scheme 2).[6] Recently, the preparation of the parent (benz)imidazole-type pNHC complexes through oxidative addition of 2-halogenoazoles to a zerovalent transition-metal center was reported by the group of Hahn (Scheme 2).[7]

The N-substituent (R in Scheme 1 B) is expected to be crucial for the tuning of the stereoelectronic properties and the coor-

[a] F. He, Dr. M. Wesolek, Dr. A. A. Danopoulos, Dr. P. Braunstein
Laboratoire de Chimie de Coordination
Institut de Chimie (UMR 7177 CNRS)
Université de Strasbourg, 4 rue Blaise Pascal
67081 Strasbourg Cedex (France)
E-mail: braunstein@unistra.fr

[b] Dr. A. A. Danopoulos
Université de Strasbourg Institute for Advanced Study (USIAS)
4 rue Blaise Pascal, 67081 Strasbourg Cedex (France)
E-mail: danopoulos@unistra.fr

[**] NHC = N-heterocyclic carbene.

Supporting information for this article is available on the WWW under http://dx.doi.org/10.1002/chem.201504030.

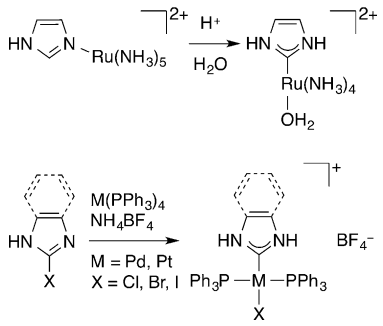

Scheme 2. Examples of transition-metal complexes containing 1*H*-(benz)imidazol-2-ylidenes.[6,7]

dination behavior of the pNHCs as well as for the stability and catalytic properties of the resulting metal complexes.[8] In most pNHC complexes, the R substituent is an alkyl or an aryl group, but there are relatively few examples where a donor functional group is attached to the N substituent that could potentially be involved in chelate formation. The number of complexes with functionalized pNHCs is still limited, and some have found catalytic applications (Scheme 3).

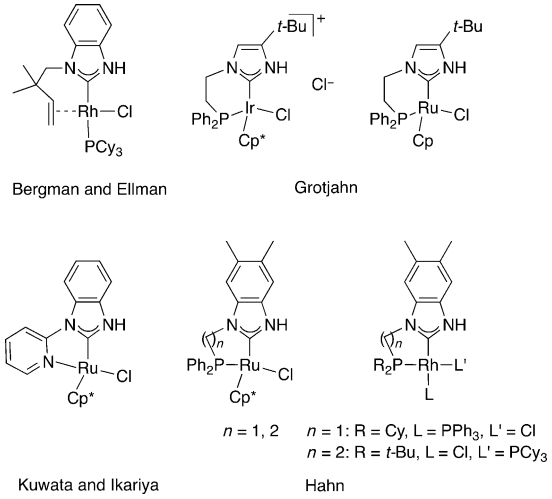

Scheme 3. Transition-metal complexes with bidentate functionalized pNHCs. Cy = cyclohexyl, Cp* = 1,2,3,4,5-pentamethylcyclopentadiene, Cp = cyclopentadiene.

Thus, Bergman et al. reported an intramolecular coupling reaction sequence of alkenes to 2-functionalized azole derivatives, in which an alkene-functionalized pNHC Rh^{I} complex was isolated as an intermediate (Scheme 3).[9] This intramolecular reaction was extended to an intermolecular coupling reaction.[10] The pyridyl-functionalized pNHC Ru^{II} complex reported by Kuwata et al. (Scheme 3) was used as a catalyst for the dehydrative condensation of *N*-(2-pyridyl)benzimidazole and allyl alcohol.[11] The phosphorus-functionalized pNHC Ir^{III} and Ru^{II} complexes reported by Grotjahn et al. (Scheme 3) were developed as catalysts for the activation of dihydrogen and in various transfer hydrogenation reactions.[12] Related phosphorus-functionalized pNHC Ru^{II}[13] and Rh^{I}[14] complexes have been reported by Hahn et al., the former revealed intermolecular hydrogen bonding between the N–H group and the 1,3-dimethyltetrahydropyrimidin-2(1*H*)-one acting as hydrogen-bond acceptor. This property appears to be common and could be utilized for substrate recognition and regioselective catalysis with pNHC complexes.[3b,c]

In view of the remarkable catalytic properties of α-diimine and pyridine diimine complexes,[15] it appeared attractive to design metal complexes bearing imine-functionalized NHC ligands.[16] The features of the imino–NHCs as hybrid ligands are based on the association of a σ-donor/π-acceptor imine and a strong σ-donor/poor π-acceptor NHC functionality. It is noteworthy that an imine-functionalized NHC Rh^{I} complex shows high activity and *cis*-selectivity in the catalytic cyclopropanation of alkenes,[17] and that imine-functionalized pNHC complexes are potentially bifunctional catalysts.[18]

We have recently demonstrated[19] that the reaction of 1-(2,6-diisopropylphenylimino)ethylimidazole ($H^{C2}\mathbf{L}$)[16f] (where the superscript associated with "H" indicates its position in the ring) with 0.5 equivalent of $[Ir(cod)(\mu\text{-}Cl)]_2$ (cod = 1,5-cyclooctadiene) afforded $[Ir(cod)Cl\{C_3H_3N_2(DippN{=}CMe)\text{-}\kappa N3\}]$ (**1a**) (Dipp = 2,6-diisopropylphenyl), abbreviated as $[Ir(cod)Cl(H^{C2}\mathbf{L}^{N3})]$ where "$\mathbf{L}^{N3}$" represents an N3-metalated, functionalized imidazole (the superscript associated with "**L**" indicates the site(s) of metalation) (Scheme 4).

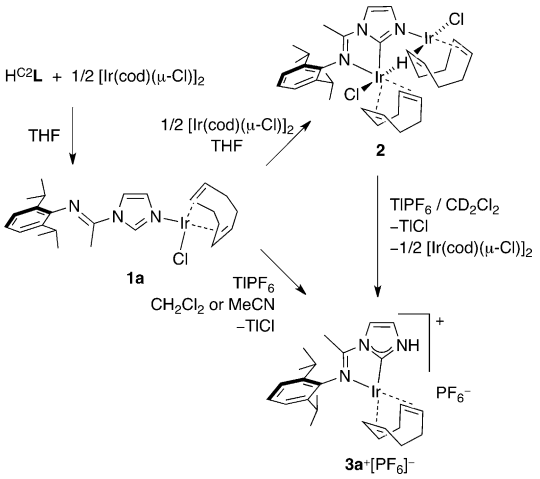

Scheme 4. Tautomerism/metallotropism leading to the pNHC complex **3a**$^{+}[PF_6]^{-}$.[19]

Reaction of complex **1a** with an additional half equivalent of $[Ir(cod)(\mu\text{-}Cl)]_2$, or the direct reaction of $H^{C2}\mathbf{L}$ with one equivalent of $[Ir(cod)(\mu\text{-}Cl)]_2$, afforded $[Ir_2(cod)_2HCl_2\{\mu\text{-}C_3H_2N_2(DippN{=}CMe)\text{-}\kappa^2(C2,N_{imine}),\kappa N3\}]$ (**2**), abbreviated as $[Ir_2(cod)_2HCl_2(\mathbf{L}^{C2,Nimine,N3})]$, which represents a mixed-valence homodinuclear complex comprising one N-bound Ir^{I} center and one $C2,N_{imine}$-chelated Ir^{III} center. The imine-functionalized pNHC Ir^{I} complex $[Ir(cod)\{C_3H_3N_2(DippN{=}CMe)\text{-}\kappa^2(C2,N_{imine})\}]^{+}[PF_6]^{-}$ (**3a**$^{+}[PF_6]^{-}$), abbreviated as $[Ir(cod)(H^{N3}\mathbf{L}^{C2,Nimine})]^{+}[PF_6]^{-}$, was obtained from the reaction of either complex **1a** or complex **2** with $TlPF_6$ (Scheme 4).[19]

Here, we further investigate the synthesis and reactivity of imine-functionalized pNHC iridium complexes by the metalation of the C2–H bond in N-bonded imidazole iridium complexes, and extend these studies to rhodium and to homo- and heterodinuclear complexes.

Results and Discussion

Chelate assistance by the imine functionality in the C2-metallation of Ir imidazole complexes

In order to examine the influence of the potentially chelating imino group on the reactivity of complex **1a**, in particular in the course of the chloride abstraction which led to products arising from tautomerization/metallotropism, we prepared the complexes [Ir(cod)Cl{$C_3H_3N_2$(*n*Bu)-κN3}] (**4a**) and [Ir(cod)-Cl{$C_3H_3N_2$(Mes)-κN3}] (**4b**)[20] (Mes = mesityl) (Scheme 5), with the *N*-butyl- and *N*-mesityl-substituents, respectively.

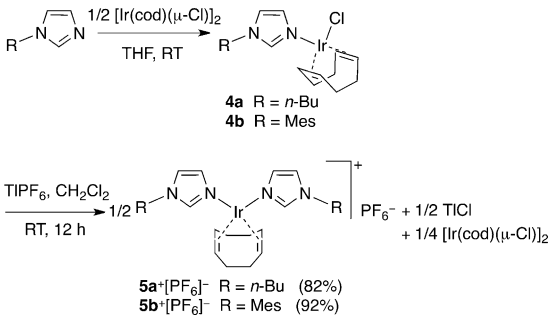

Scheme 5. Synthesis of complexes **4a** and **4b** as well as complexes **5a**$^+$[PF_6]$^-$ and **5b**$^+$[PF_6]$^-$.

Under conditions similar to those used for the chloride abstraction reaction of complex **1a**, complexes **4a** and **4b** only afforded the complexes [Ir(cod){$C_3H_3N_2$(R)-κN3}$_2$]$^+$[PF_6]$^-$ [i.e., **5a**$^+$[PF_6]$^-$ (R = *n*Bu), **5b**$^+$[PF_6]$^-$ (R = Mes)]; this was evidenced by the ratio of the coordinated imidazoles and the 1,5-cyclooctadiene (2:1) in the ^{1}H NMR spectra. The reaction was accompanied by the formation of [Ir(cod)(μ-Cl)]$_2$ (NMR evidence). These results point to the crucial role of the N-arylimino functional group for the tautomerization/metallotropism manifested by the conversion of the N-bound Ir^I to the Ir^I–pNHC complex (Scheme 4).

In comparison, although the formation of [Ir(cod)-{$C_3H_3N_2$(DippN=CMe)-κN3}$_2$]$^+$[PF_6]$^-$ (**6a**$^+$[PF_6]$^-$), abbreviated as [Ir(cod)(H^{C2}**L**^{N3})$_2$]$^+$[PF_6]$^-$, was observed in the initial stages of the halide abstraction reaction from complex **1a**, as evidenced by monitoring the reaction of the latter with $TlPF_6$ in CD_2Cl_2 at room temperature by ^{1}H NMR spectroscopy, it could not be isolated. Informatively, we show below that complex **6a**$^+$[PF_6]$^-$ can further react with [Ir(cod)(μ-Cl)]$_2$ to give complex **3a**$^+$[PF_6]$^-$ (see Scheme 8). In contrast to complexes **5a**$^+$[PF_6]$^-$ and **5b**$^+$[PF_6]$^-$ (Scheme 5), complex **1a** was fully converted to complex **3a**$^+$[PF_6]$^-$ at the end of the reaction (Scheme 4). Addition of one equivalent of H^{C2}**L** was required in order to isolate complex **6a**$^+$[PF_6]$^-$ (Scheme 6).

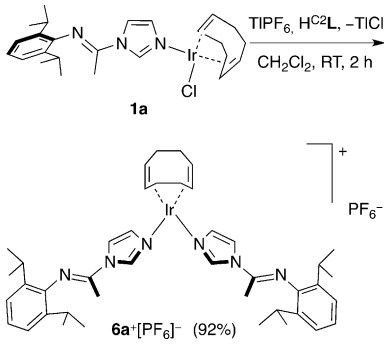

Scheme 6. Synthesis of complex **6a**$^+$[PF_6]$^-$.

In the ^{1}H NMR spectrum, the 2:1 ratio between the imidazole and the 1,5-cod protons in complex **6a**$^+$[PF_6]$^-$ is consistent with the molecular structure of complex **6a**$^+$[PF_6]$^-$ in the solid state (Figure 1). The sixteen valence-electron iridium center in complex **6a**$^+$[PF_6]$^-$ adopts an approximate square-planar coordination geometry, defined by the two olefinic bonds of the 1,5-cod ligand and two nitrogen atoms from the imidazole ligands.

Complexes with functionalized pNHC ligands, related to complex **3a**$^+$[PF_6]$^-$, and bearing bidentate (benz)imidazolin-2-ylidene/donor ligands, have been obtained by formal tautomerization/metallotropism,[11–13] Hahn et al. proposed the occurrence of a "redox tautomerization" involving an initial C2–H oxidative addition of azoles followed by reductive elimination of the proton on the metal center.[3b,14,21]

In the present case of the tautomerization of complex **1a** to complex **3a**$^+$[PF_6]$^-$, we suggest on the basis of ^{1}H NMR monitoring that complex **2** (Scheme 4) is a reaction intermediate. It was isolated in an separate experiment and can be viewed as the product of a C2–H oxidative addition of the N-bound iridium complex **1a** (Scheme 4), requiring the presence of a catalytic amount of [Ir(cod)(μ-Cl)]$_2$. Then, ^{1}H NMR monitoring of the reaction between complex **2** and $TlPF_6$ in CD_2Cl_2 (Scheme 4) re-

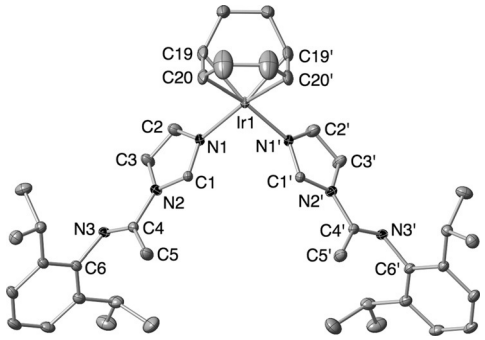

Figure 1. Molecular structure of the cation in complex **6a**$^+$[PF_6]$^-$. Hydrogen atoms are omitted for clarity. Thermal ellipsoids are at the 30% level. The crystallographic labels C1 and N1 correspond to the conventional C2 and N3 numbering used in the text. Selected bond lengths [Å] and angles [°]: C1–N1 1.322(5), C1–N2 1.363(5), C2–N1 1.393(5), C2–C3 1.352(6), C3–N2 1.379(5), C4–N2 1.435(4), C4–N3 1.255(5), C4–C5 1.491(5), C6–N3 1.422(4), Ir1–N1 2.078(3), Ir1–C19 2.125(5), Ir1–C20 2.120(5), C19–C20 1.391(9); N1-C1-N2 110.2(3), N1-Ir1-C19 91.8(2), N1-Ir1-C20 92.3(2), N1-Ir1-N1′ 88.3(2).

vealed a hydride resonance at $\delta = -14.41$ ppm, which could be tentatively assigned to the intermediate $[\mathbf{2}-Cl^-]^+[PF_6]^-$ in cycle I (compare $\delta = -15.12$ ppm in complex **2**). In a ^1H NMR experiment for monitoring the chloride abstraction of complex **1a** with $TlPF_6$ in CD_2Cl_2 at room temperature, the resonances of complex $\mathbf{6a}^+[PF_6]^-$ and of three hydride species were observed in the initial stages of the reaction, in a ratio of approximately 1:20:4 at $\delta = -14.41$ ($[\mathbf{2}-Cl^-]^+[PF_6]^-$), -14.99, -15.12 ppm (**2**) (Figure S1 in the Supporting Information), respectively, which progressively disappeared. The hydride species observed at $\delta = -14.41$ ($[\mathbf{2}-Cl^-]^+[PF_6]^-$) and -15.12 ppm (**2**) are consistent with the suggested steps shown in cycle I of Scheme 7.

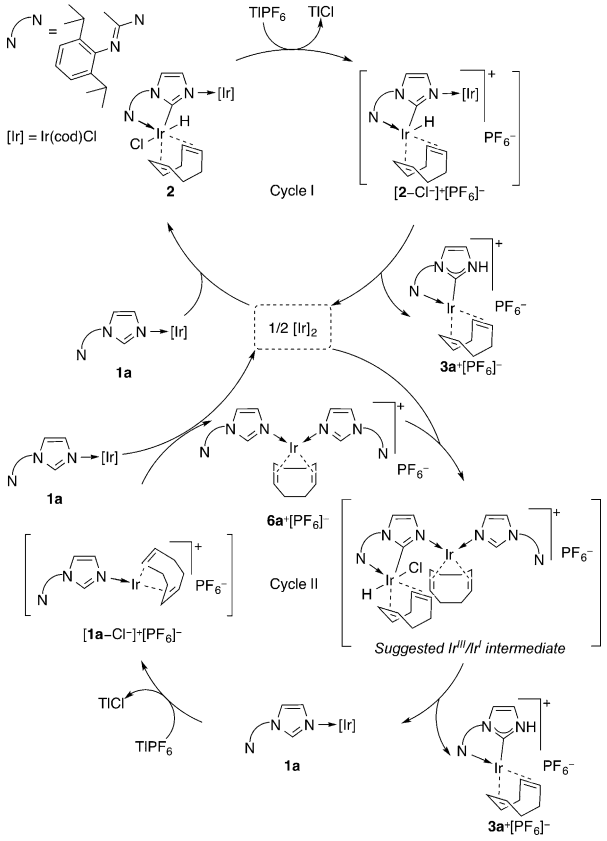

Scheme 7. Proposed mechanism for the tautomerization of complex **1a** to complex $\mathbf{3a}^+[PF_6]^-$ through a neutral and a cationic Ir^{III}/Ir^{I} intermediate.

In order to prove that C2–H bond activation can occur on the N3-coordinated imidazole in complexes of the type $[Ir(cod)(H^{C2}\mathbf{L}^{N3})_2]^+$ (compare behavior of complexes **4a** and **4b** giving complexes $\mathbf{5a}^+$ and $\mathbf{5b}^+$, respectively, Scheme 5), a reaction between complexes $\mathbf{6a}^+[PF_6]^-$ and $[Ir(cod)(\mu\text{-}Cl)]_2$ in CD_2Cl_2 was monitored by ^1H NMR spectroscopy (Scheme 8). Interestingly, we observed the same intermediate hydride species as in the chloride abstraction reaction of complex **1a** (Figure S2 in the Supporting Information). These postulated steps for the tautomerization of complex **1a** to complex $\mathbf{3a}^+[PF_6]^-$ are summarized in cycle II of Scheme 7. Furthermore, the observation of complexes **1a** and $\mathbf{3a}^+[PF_6]^-$ indicates that complex $\mathbf{6a}^+[PF_6]^-$ is an intermediate in the tautomerization of complex **1a** to complex $\mathbf{3a}^+[PF_6]^-$ and therefore, cannot be isolated by this sequence of steps.

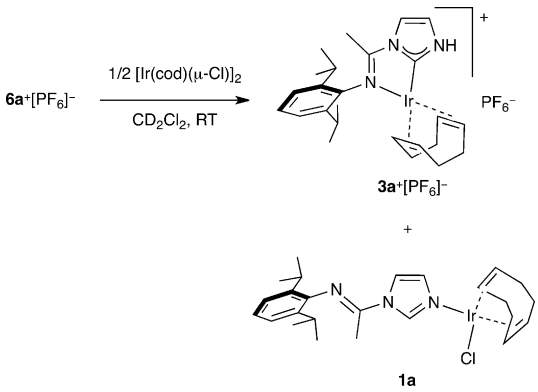

Scheme 8. The reaction between complexes $\mathbf{6a}^+[PF_6]^-$ and $[Ir(cod)(\mu\text{-}Cl)]_2$ that was monitored by ^1H NMR spectroscopy.

The reaction between complex **1a** and $TlPF_6$ (cycle II in Scheme 7) would give a reactive Ir species, that is, $[\mathbf{1a}-Cl^-]^+[PF_6]^-$, which could react with complex **1a** still present to yield complex $\mathbf{6a}^+[PF_6]^-$ by ligand transfer, and $[Ir(cod)(\mu\text{-}Cl)]_2$. The latter could activate the C2–H bond either of complex **1a** to give complex **2** (cycle I in Scheme 7) or of complex $\mathbf{6a}^+[PF_6]^-$ to give complex $\mathbf{3a}^+[PF_6]^-$ (Scheme 8 and cycle II in Scheme 7), through a postulated Ir^{III}/Ir^{I} intermediate, which is supposed to be the hydride species resonating at $\delta = -14.99$ ppm. Proton transfer from the Ir^{III} center to the N3 atom of the metalated heterocycle with concomitant breaking of the N3–Ir^{I} bond would lead to complexes $\mathbf{3a}^+[PF_6]^-$ and **1a**, the latter remaining in the cycle until complete conversion to complex $\mathbf{3a}^+[PF_6]^-$. In summary, the species postulated in cycles I and II in Scheme 7 point to the different elementary steps that lead to tautomerization (H-shift) and "apparent" metallotropism (Ir-to-N3 shift), the latter formally involving different iridium species.

With the aim to explore the scope of the H-shift from N to Ir in pNHCs as a way to access valence tautomers, we reacted complex $\mathbf{3a}^+[PF_6]^-$ with phosphine ligands to render the metal center more electron-rich, hoping to favor a transformation from Ir^{I} to Ir^{III}. Addition of triphenylphosphine/trimethylphosphine afforded the eighteen-valence-electron addition products $[Ir(cod)(PR_3)\{C_3H_3N_2(DippN{=}CMe)\text{-}\kappa^2(C2,N_{imine})\}]^+[PF_6]^-$ ($\mathbf{7a}^+[PF_6]^-$ (R = Ph) and $\mathbf{7b}^+[PF_6]^-$ (R = Me)), abbreviated as $[Ir(cod)(PR_3)(H^{N3}\mathbf{L}^{C2,Nimine})]^+[PF_6]^-$ (Scheme 9).

In the $^{31}P\{^1H\}$ NMR spectrum of complex $\mathbf{7a}^+[PF_6]^-$, the PPh_3 ligand gives rise to a singlet at $\delta = -1.9$ ppm. In complex $\mathbf{7b}^+[PF_6]^-$, a characteristic $^{31}P\{^1H\}$ NMR singlet peak at $\delta = -44.8$ ppm and the C_{NHC} resonance at $\delta = 171.1$ ppm (d, $^2J(P,C) = 10.9$ Hz) in the $^{13}C\{^1H\}$ NMR spectrum suggest that coordination of the PMe_3 ligand occurs in *cis* position to the C_{NHC} atom. In the structure of complex $\mathbf{7a}^+[PF_6]^-$ (Figure 2), the iridium center adopts a distorted trigonal-bipyramidal coordination geometry, with the C1 atom and the C22=C23 double bond in the apical positions.[22] The Ir1–C1 bond length in

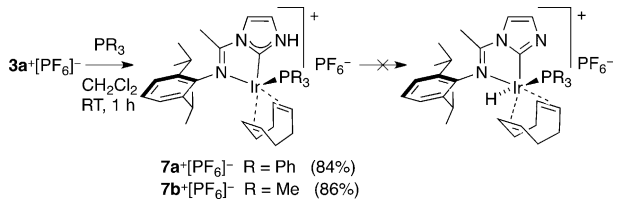

Scheme 9. Synthesis of complexes **7a**$^+$[PF_6]$^-$ and **7b**$^+$[PF_6]$^-$.

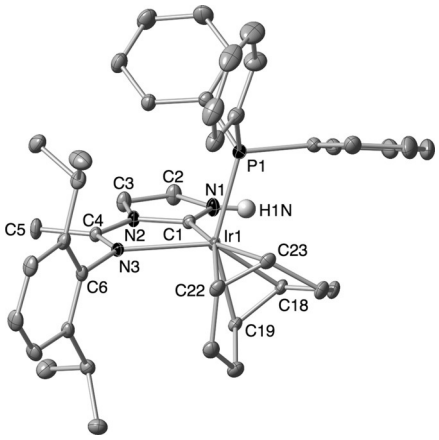

Figure 2. Molecular structure of the cation in complex **7a**$^+$[PF_6]$^-$. Hydrogen atoms are omitted for clarity, except H1N. Thermal ellipsoids are at the 30% level. Selected bond lengths [Å] and angles [°]: C1–N1 1.345(2), C1–N2 1.371(2), C2–N1 1.388(3), C2–C3 1.337(3), C3–N2 1.402(2), C4–N2 1.402(2), C4–N3 1.284(2), C4–C5 1.495(3), C6–N3 1.453(2), Ir1–P1 2.3388(5), Ir1–C1 1.982(2), Ir1–N3 2.347(2), Ir1–C18 2.118(2), Ir1–C19 2.142(2), Ir1–C22 2.220(2), Ir1–C23 2.269(2), C18–C19 1.445(3), C22–C23 1.390(3), N1–H1N 0.82(3); N1-C1-N2 104.0(2), C1-Ir1-N3 73.61(6), C1-Ir1-P1 89.59(5), C1-Ir1-C18 89.36(7), C1-Ir1-C19 90.85(8), N3-Ir1-P1 108.63(4).

complex **7a**$^+$[PF_6]$^-$ (1.982(2) Å) is similar to that in complex **3a**$^+$[PF_6]$^-$ (1.984(3) Å), but the Ir1–N3 bond in complex **7a**$^+$[PF_6]$^-$ is considerably longer than the corresponding bond in complex **3a**$^+$[PF_6]$^-$ (2.347(2) vs. 2.115(3) Å), which is consistent with the respective electron counts of the metals and the steric hindrance in complex **7a**$^+$. The closest N–H···F(PF_5) distance of 2.21(3) Å is consistent with a hydrogen-bonding interaction. Although as expected, phosphine coordination has taken place in the reactions given in Scheme 9, a transformation from Ir^I to Ir^{III} species was not observed in these reactions, in contrast to findings involving a 1,9-phenanthroline-derived pNHC system.[22c] The stability of complexes **7a**$^+$[PF_6]$^-$ and **7b**$^+$[PF_6]$^-$ is consistent with their eighteen-valence-electron count.

To further study the possible contribution of the imino group on the tautomerization/metallotropism, the ligand H^{C2}**L**′, which is a derivative of H^{C2}**L**, was designed in which the carbon atoms C5 and C4 of the heterocycle are substituted by methyl and imino groups in order to prevent the formation of abnormal NHC complexes and to provide chelate assistance by imine coordination, respectively. Reaction of H^{C2}**L**′ with [Ir(cod)(μ-Cl)]$_2$ led to the formation of [Ir(cod)Cl{C_3HN_2(DippN=CMe)(DippN=CH)(Me)-κN3}] (**8**), abbreviated as [Ir(cod)-Cl(H^{C2}**L**′^{N3})] (Scheme 10).

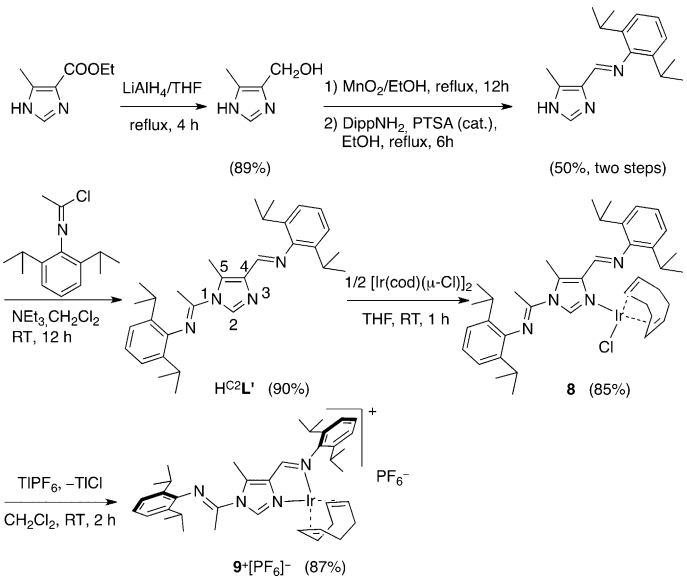

Scheme 10. Synthesis of the ligand H^{C2}**L**′ and complexes **8** and **9**$^+$[PF_6]$^-$. PTSA = *p*-toluenesulfonic acid.

Abstraction of the chloride ligand from complex **8** in CH_2Cl_2 did not lead to "Ir migration" from N to C2, but to rapid chelation of the proximal imino group to give [Ir(cod)-{C_3HN_2(DippN=CMe)(DippN=CH)(Me)-κ^2(N3,N_{imine})}]$^+$[PF_6]$^-$ (**9**$^+$[PF_6]$^-$), abbreviated as [Ir(cod)(H^{C2}**L**′^{N3,Nimine})]$^+$[PF_6]$^-$, the structure of which was confirmed crystallographically (Figure 3). In contrast to complex **1a**, which can lead to the dinuclear Ir^{III}/Ir^I complex **2** (Scheme 4), complex **9**$^+$[PF_6]$^-$ does not react further with [Ir(cod)(μ-Cl)]$_2$, possibly for steric reasons, the orientation of the Ir(cod) moiety being locked owing to N,N chelation.

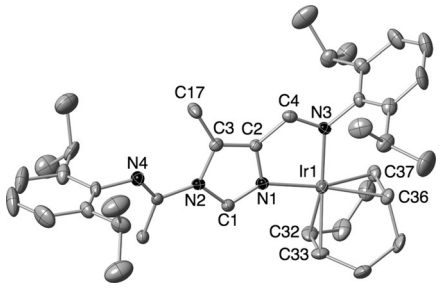

Figure 3. Molecular structure of the cation in **9**$^+$[PF_6]$^-$. Hydrogen atoms are omitted for clarity. Thermal ellipsoids are at the 30% level. Selected bond lengths [Å] and angles [°]: C1–N1 1.31(1), C1–N2 1.38(1), C2–N1 1.394(9), C2–C3 1.37(1), C3–N2 1.41(1), C4–N3 1.31(1), Ir1–N1 2.083(7), Ir1–N3 2.094(6), Ir1–C32 2.154(9), Ir1–C33 2.137(8), Ir1–C36 2.110(9), Ir1–C37 2.123(9), C32–C33 1.43(2), C36–C37 1.38(1); N1-C1-N2 111.1(7), N1-Ir1-N3 78.9(3), N1-Ir1-C32 98.6(3), N1-Ir1-C33 94.2(3), N3-Ir1-C36 97.5(3), N3-Ir1-C37 93.6(3).

Synthesis of imine-functionalized pNHC Rh^I complexes

Similarly to complex **1a**, the reaction of the ligand H^{C2}**L** with 0.5 equivalent of [Rh(cod)(μ-Cl)]$_2$ in THF gave [Rh(cod)Cl{$C_3H_3N_2$(DippN=CMe)-κN3}] (**1b**), abbreviated as [Rh(cod)Cl(H^{C2}**L**^{N3})], in nearly quantitative yield (Scheme 11).

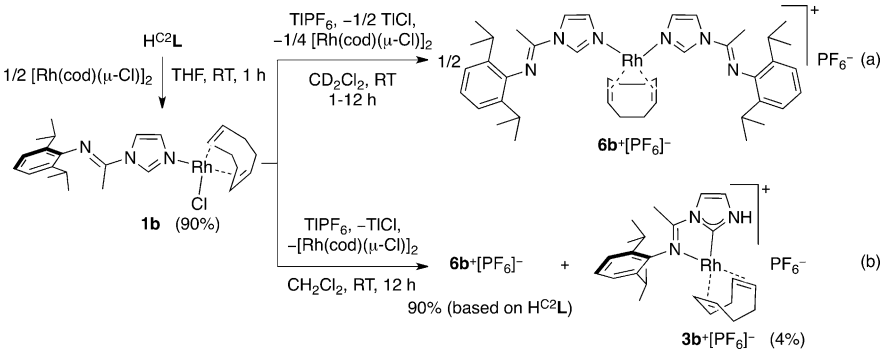

Scheme 11. Synthesis of the Rh^{I} complexes **1 b**, **3 b**$^{+}[PF_6]^{-}$, and **6 b**$^{+}[PF_6]^{-}$.

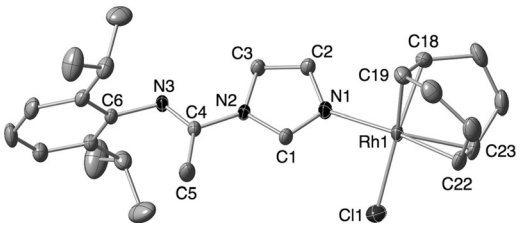

Figure 4. Molecular structure of complex **1 b**. Hydrogen atoms are omitted for clarity. Thermal ellipsoids are at the 30% level. Selected bond lengths [Å] and angles [°]: C1–N1 1.315(2), C1–N2 1.359(2), C2–N1 1.383(2), C2–C3 1.355(2), C3–N2 1.381(2), C4–N2 1.428(2), C4–N3 1.260(2), C4–C5 1.496(2), C6–N3 1.428(2), Rh1–N1 2.104(1), Rh1–Cl1 2.3748(5), Rh1–C18 2.120(2), Rh1–C19 2.101(2), Rh1–C22 2.143(2), Rh1–C23 2.127(2), C18–C19 1.399(3), C22–C23 1.396(3); N1-C1-N2 111.1(1), N1-Rh1-Cl1 88.36(4), N1-Rh1-C18 93.69(6), N1-Rh1-C19 90.02(6), Cl1-Rh1-C22 92.20(6), Cl1-Rh1-C23 91.16(6).

In the ^{1}H NMR spectrum of complex **1 b** in CD_2Cl_2, the C2–H exhibits a broad singlet at $\delta = 8.73$ ppm (compare $\delta =$ 8.11 ppm in the ligand H^{C2}**L**). The molecular structure of complex **1 b** is shown in Figure 4.

Defined by the two double bonds of the 1,5-cod ligand, one nitrogen atom of the imidazole, and one terminal chloride ligand, the rhodium center adopts a distorted square-planar coordination geometry, as evidenced by the bond angles at Rh, namely, N1-Rh1-Cl1 88.36(4), N1-Rh1-C18/C19 93.69(6)/90.02(6), and Cl1-Rh1-C22/C23 92.20(6)/91.16(6)°. This is consistent with the IR absorption band at $\tilde{\nu} = 1685$ cm^{-1} assigned to the ν(C=N) vibration of the dangling imino functionality and the $^{13}C\{^{1}H\}$ NMR signal at $\delta = 149.0$ ppm assigned to the C=N moiety.

Inspired by the conversion of complex **1 a** to complex **3 a**$^{+}[PF_6]^{-}$, we investigated analogous reactivity with the rhodium complex **1 b**. In a ^{1}H NMR monitoring experiment, the reaction of complex **1 b** with 1.0 equivalent of $TlPF_6$ in CD_2Cl_2 at room temperature gave a white precipitate of TlCl and a yellow solution, which (as proven by ^{1}H NMR spectroscopy) contained half one equivalent of a new rhodium species, that is, [Rh(cod){$C_3H_3N_2$(DippN=CMe)-κN3}$_2$]$^{+}[PF_6]^{-}$ (**6 b**$^{+}[PF_6]^{-}$), abbreviated as [Rh(cod)(H^{C2}**L**^{N3})$_2$]$^{+}[PF_6]^{-}$, and 0.25 equivalent of [Rh(cod)(μ-Cl)]$_2$ resulting from a ligand transfer reaction, but no pNHC Rh complex was detected (Scheme 11 a). However, when this experiment was repeated on a larger scale in dichloromethane at room temperature, the color of the solution slightly turned to red and the pNHC Rh^{I} complex [Rh(cod){$C_3H_3N_2$(DippN=CMe)-κ^2(C2,N_{imine})}]$^{+}[PF_6]^{-}$ (**3 b**$^{+}[PF_6]^{-}$), abbreviated as [Rh(cod)(H^{N3}**L**^{C2,Nimine})]$^{+}[PF_6]^{-}$, was isolated in 4% yield as dark red crystals by fractional crystallization (Scheme 11 b) (see the Experimental Section). The low yield partly explains why complex **3 b**$^{+}[PF_6]^{-}$ had not been observed in the ^{1}H NMR experiment. From the supernatant solution, complex **6 b**$^{+}[PF_6]^{-}$ was isolated as a pale yellow powder in good yield (90% based on H^{C2}**L**). The ^{1}H NMR data of complex **6 b**$^{+}[PF_6]^{-}$ in CD_2Cl_2 established the ratio of the imidazole and the 1,5-cod ligands to be 2:1 and the upfield shift by 0.31 ppm (compared to complex **1 b)** of the resonance of the C2–H proton at $\delta = 8.42$ ppm. In the ^{13}C NMR spectrum, the resonance at $\delta = 137.0$ ppm was assigned to the C2–H carbon atom. The IR band for the ν(C=N) vibration of a dangling imine group in complex **6 b**$^{+}[PF_6]^{-}$ was observed at $\tilde{\nu} = 1687$ cm^{-1}.

In the ^{1}H NMR spectrum of complex **3 b**$^{+}[PF_6]^{-}$ in CD_2Cl_2, the N–H proton appears as a broad singlet at $\delta = 10.31$ ppm and the $^{13}C\{^{1}H\}$ NMR spectrum contains resonances for the $C2_{NHC}$ and C_{imine} carbon atoms at $\delta = 176.9$ (d, ^{1}J(Rh,C) = 55.1 Hz) and 163.7 ppm, respectively (compare $\delta = 138.6$ and 149.0 ppm, respectively, in complex **1 b**). The IR absorptions at $\tilde{\nu} = 3405$ and 1627 cm^{-1} can be assigned to N–H[19, 22c, 23] and coordinated C=N stretching vibrations, respectively. All these data indicate that complex **3 b**$^{+}[PF_6]^{-}$ is a κ^2(C2,N_{imine})-chelated imino–NHC rhodium complex, which was further confirmed crystallographically (Figure 5).

In the structure of complex **3 b**$^{+}[PF_6]^{-}$, the square-planar coordination geometry around the metal center, which is defined by the κ^2(C2,N_{imine}) five-membered ring chelate and the two olefinic bonds of the 1,5-cod ligand, is strongly distorted, with an acute C1-Rh1-N3 angle of 77.7(1)°. In agreement with a lower *trans* influence of the imino group compared to the NHC donor, the Rh1–C18/C25 (2.137(3)/2.122(3) Å) bond lengths are shorter than the Rh1–C21/C22 (2.239(3)/2.256(3) Å) bond length and, consistently, the C18=C25 double bond (1.390(5) Å) is slightly longer than the C21=C22 (1.345(5) Å) double bond, owing to increased back-bonding from the metal. The Rh–C_{NHC} bond length of 1.972(3) Å is similar to that found in the κ^2(C2,N_{imine})-chelated imino–NHC rhodium complex with a N-methyl substituent (1.99(1) Å).[17b] Owing to the coordination of the N_{imine} atom to the Rh atom, the C4–N3

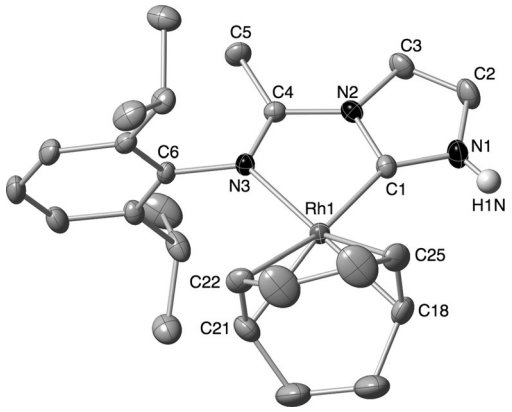

Figure 5. Molecular structure of the cation in complex $\mathbf{3b}^{+}[PF_6]^{-}$. Hydrogen atoms are omitted for clarity, except H1N. Thermal ellipsoids are at the 30% level. Selected bond lengths [Å] and angles [°]: C1–N1 1.342(4), C1–N2 1.369(4), C2–N1 1.380(4), C2–C3 1.340(5), C3–N2 1.392(3), C4–N2 1.399(3), C4–N3 1.287(3), C4–C5 1.484(4), C6–N3 1.444(3), Rh1–C1 1.972(3), Rh1–N3 2.125(2), Rh1–C18 2.137(3), Rh1–C21 2.239(3), Rh1–C22 2.256(3), Rh1–C25 2.122(3), C18–C25 1.390(5), C21–C22 1.345(5), N1–H1N 0.82(4); N1-C1-N2 103.0(2), C1-Rh1-N3 77.7(1), C1-Rh1-C18 95.9(1), C1-Rh1-C25 94.8(1), N3-Rh1-C21 100.6(1), N3-Rh1-C22 97.9(1).

bond in complex $\mathbf{3b}^{+}[PF_6]^{-}$ (1.287(3) Å) is longer than that in complex **1b** (1.260(2) Å), whereas the C4–N2 bond in complex $\mathbf{3b}^{+}[PF_6]^{-}$ (1.399(3) Å) is shorter than that in complex **1b** (1.428(2) Å). As expected from the decreased π delocalization over the azole ring, the bond lengths of the C1–N1/N2 bonds in complex $\mathbf{3b}^{+}[PF_6]^{-}$ (1.342(4)/1.369(4) Å) are longer than those in complex **1b** (1.321(2)/1.359(2) Å). As a result, the N1-C1-N2 bond angle in complex $\mathbf{3b}^{+}[PF_6]^{-}$ (103.0(2)°) is also significantly less obtuse than that in complex **1b** (111.1(1)°). The shortest N–H···F(PF_5) distances of 2.43(4) and 2.49(4) Å are consistent with hydrogen-bonding interactions.

In an attempt to improve the yield of complex $\mathbf{3b}^{+}[PF_6]^{-}$, we used toluene as the reaction solvent. In a ^{1}H NMR experiment in [D_8]toluene at room temperature, the reaction of complex **1b** with one equivalent of $TlPF_6$ was found to give the same products as in CD_2Cl_2. However, after heating the reaction mixture to 110 °C for twelve hours, the yellow solution became colorless and a red precipitate was formed. The ^{1}H NMR spectroscopic data of the solution indicated complete consumption of complexes $\mathbf{6b}^{+}[PF_6]^{-}$ and [Rh(cod)(μ-Cl)]$_2$. The red precipitate was isolated by filtration and extracted in CD_2Cl_2 giving pure $\mathbf{3b}^{+}[PF_6]^{-}$ in solution and a white precipitate of TlCl. Repeating the reaction on a larger scale led to the isolation of complex $\mathbf{3b}^{+}[PF_6]^{-}$ in 90% yield (Scheme 12).

When a solution of complex $\mathbf{6b}^{+}[PF_6]^{-}$, in the presence or not of 0.5 equivalent of [Rh(cod)(μ-Cl)]$_2$, was heated at 110 °C for more than 24 hours, no $\mathbf{3b}^{+}[PF_6]^{-}$ was observed but only a slight decomposition of complex $\mathbf{6b}^{+}[PF_6]^{-}$ occurred (Scheme 12). These results suggest that complex $\mathbf{6b}^{+}[PF_6]^{-}$ is an intermediate in the synthesis of complex $\mathbf{3b}^{+}[PF_6]^{-}$ only in the presence of both [Rh(cod)(μ-Cl)]$_2$ and $TlPF_6$ (compare the corresponding Ir complexes described above).

The tautomerization of complex **1b** to complex $\mathbf{3b}^{+}[PF_6]^{-}$ may apparently proceed similarly to the conversion of complex

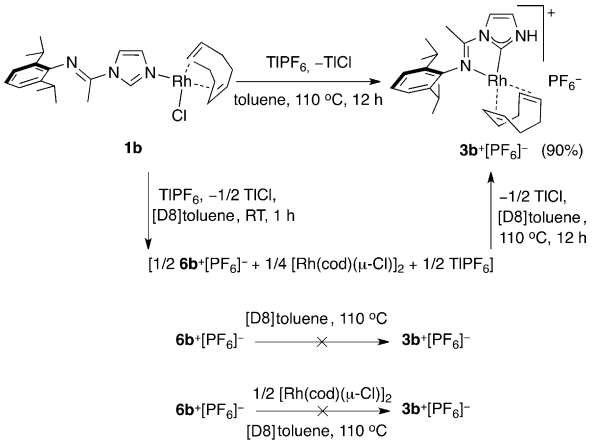

Scheme 12. Improved synthesis of complex $\mathbf{3b}^{+}[PF_6]^{-}$.

1a to complex $\mathbf{3a}^{+}[PF_6]^{-}$, but a different mechanism may be operative because Rh–H species were not detected in situ by ^{1}H NMR spectroscopy, although this may be attributable to the poor solubility of the cationic hydride species in [D_8]toluene.

Homo- and heterodinuclear Ir and Rh complexes

To expand the scope and the reactivity of complexes **1a** and $\mathbf{3a}^{+}[PF_6]^{-}$, we considered to use them as precursors for dinuclear complexes. The in situ deprotonation of complex **1a** by potassium bis(trimethylsilyl)amide (KHMDS) in THF at −30 °C initially gave a red solution; after addition of 0.5 equivalent of [Ir(cod)(μ-Cl)]$_2$ the dark green [Ir$_2$(cod)$_2$Cl{μ-$C_3H_2N_2$(DippN=CMe)-κ^2(C2,N$_{imine}$),κN3}] (**10**), abbreviated as [Ir$_2$(cod)$_2$Cl-(**L**^{C2,Nimine,N3})], was isolated (Scheme 13).

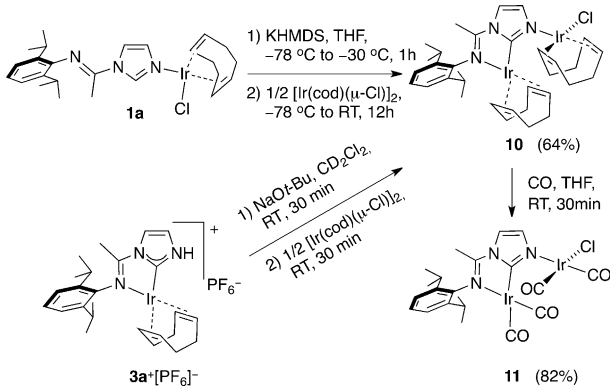

Scheme 13. Synthesis of the dinuclear Ir^{I} complexes **10** and **11**.

An IR absorption band at $\tilde{\nu}$ = 1577 cm^{-1} for the C=N stretching vibration and the ^{13}C{^{1}H} NMR resonance due to the C=N carbon atom (δ = 166.0 ppm) support the coordination of the N$_{imine}$ atom to the cationic Ir^{I} center in complex **10**. In addition, the disappearance of a C2–H resonance in the ^{1}H NMR spectrum of complex **10** (in C_6D_6), and the appearance of a signal at δ = 180.6 ppm in the ^{13}C{^{1}H} NMR spectrum, confirmed the formation of an Ir–C$_{NHC}$ bond.

The structure of complex **10**·Et_2O·toluene (Figure 6) revealed a dinuclear complex comprising one N-bound Ir^I center and one κ^2(C2,N_{imine})-chelated Ir^I center (compare the κ^2(C2,N_{imine}) chelation of the Ir^{III} center in complex **2**). Both iridium centers adopt distorted square-planar coordination geometries. In a ^{1}H NMR experiment performed in CD_2Cl_2, complex **10** was alternatively synthesized from the reaction of complex **3a**$^+[PF_6]^-$ with one equivalent of NaO*t*Bu (which led to an equilibrium between a mononuclear neutral complex containing a C-bound "anionic" imidazolide and its dimer in which the imidazolide binds in a μ-C,N bridging mode)[19] followed by the addition of 0.5 equivalent of [Ir(cod)(μ-Cl)]$_2$. The yield (by ^{1}H NMR spectroscopy) is higher than 80%.

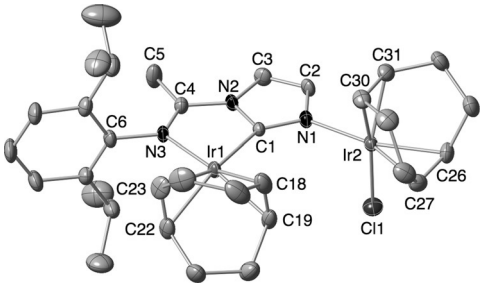

Figure 6. Molecular structure of complex **10** in **10**·Et_2O·toluene. Hydrogen atoms and the solvent molecules are omitted for clarity. Thermal ellipsoids are at the 30% level. Selected bond lengths [Å] and angles [°]: C1–N1 1.335(6), C1–N2 1.397(7), C2–N1 1.391(7), C2–C3 1.342(8), C3–N2 1.387(7), C4–N2 1.382(6), C4–N3 1.289(7), C4–C5 1.486(8), C6–N3 1.454(6), Ir1–C1 2.041(5), Ir1–N3 2.112(4), Ir1–C18 2.137(6), Ir1–C19 2.118(6), Ir1–C22 2.185(5), Ir1–C23 2.184(5), C18–C19 1.400(9), C22–C23 1.380(9), Ir2–Cl1 2.367(1), Ir2–C26 2.149(5), Ir2–C27 2.111(6), Ir2–C30 2.113(5), Ir2–C31 2.099(5), C26–C27 1.396(8), C30–C31 1.418(8); N1-C1-N2 105.9(4), C1-Ir1-N3 78.3(2), C1-Ir1-C18 100.2(2), C1-Ir1-C19 95.8(2), N3-Ir1-C22 98.4(2), N3-Ir1-C23 94.3(2), N1-Ir2-Cl1 88.1(1), N1-Ir2-C30 93.4(2), N1-Ir2-C31 91.0(2), Cl1-Ir2-C26 92.3(2), Cl1-Ir2-C27 91.6(2).

The two cod ligands in complex **10** were readily replaced by CO at room temperature to afford the red [$Ir_2(CO)_4Cl${μ-$C_3H_2N_2$(DippN=CMe)-κ^2(C2,N_{imine}),κN3}] (**11**), abbreviated as [$Ir_2(CO)_4Cl$(**L**^{C2,Nimine,N3})]. Its IR spectrum showed two strong ν(CO) bands at $\tilde{\nu}$ = 2054 (s) and 1971 cm^{-1} (vbr), which is consistent with a mutually *cis* disposition of the CO ligands, further confirmed crystallographically (Figure 7).

Unexpectedly, both the in situ deprotonation of complex **1b** by KHMDS followed by the addition of 0.5 equivalent of [Ir(cod)(μ-Cl)]$_2$ and the in situ deprotonation of complex **1a** by KHMDS followed by the addition of 0.5 equivalent of [Rh(cod)(μ-Cl)]$_2$ afforded the same heterodinuclear complex [IrRh(cod)$_2$Cl{μ-$C_3H_2N_2$(DippN=CMe) -κ^2(C2,N_{imine}),κN3}] (**12**), abbreviated as [IrRh(cod)$_2$Cl(**L**^{C2,Nimine,N3})], in 60 and 51% yield, respectively (Scheme 14).

In the ^{13}C{^{1}H} NMR spectrum of complex **12**, a characteristic singlet at δ = 179.8 ppm was assigned to the C_{NHC} carbon atom. The structure of complex **12**·2THF (Figure 8) revealed a dinuclear complex comprising one N-bound Rh^I center and one κ^2(C2,N_{imine})-chelated Ir^I center. Both metals adopt distorted square-planar coordination geometries. The reactions

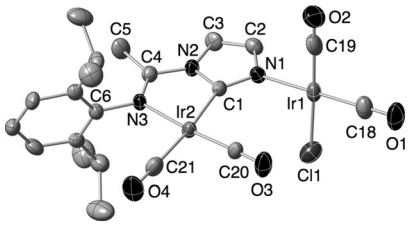

Figure 7. Molecular structure of complex **11**. Thermal ellipsoids are at the 30% level. Selected bond lengths [Å] and angles [°]: C1–N1 1.336(9), C1–N2 1.391(9), C2–N1 1.386(9), C2–C3 1.35(1), C3–N2 1.392(8), C4–N2 1.378(9), C4–N3 1.302(9), C4–C5 1.47(1), C6–N3 1.443(8), C1–Ir2 2.052(7), N3–Ir2 2.097(6), C20–Ir2 1.838(8), C21–Ir2 1.907(8), N1–Ir1 2.074(6), Cl1–Ir1 2.339(2), C18–Ir1 1.848(9), C19–Ir1 1.85(1), C18–O1 1.15(1), C19–O2 1.14(1), C20–O3 1.148(9), C21–O4 1.131(9); N1-C1-N2 106.6(6), C1-Ir2-N3 77.5(2), C1-Ir2-C20 97.6(3), C20-Ir2-C21 89.9(3), C21-Ir2-N3 95.0(3), N1-Ir1-Cl1 86.6(2), N1-Ir1-C19 91.8(3), C18-Ir1-C19 88.9(4), C18-Ir1-Cl1 92.7(3).

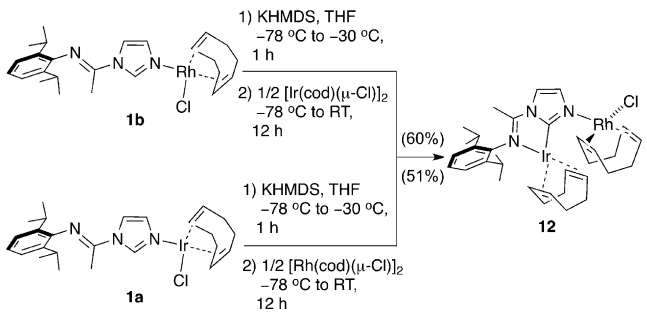

Scheme 14. Syntheses of complex **12**.

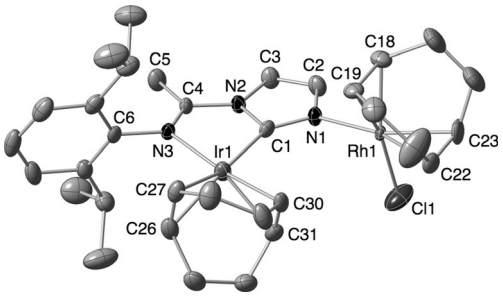

Figure 8. Molecular structure complex **12** in **12**·2THF. Hydrogen atoms and the solvent molecules are omitted for clarity. Thermal ellipsoids are at the 30% level. Selected bond lengths [Å] and angles [°]: C1–N1 1.331(7), C1–N2 1.418(7), C2–N1 1.392(8), C2–C3 1.349(9), C3–N2 1.387(7), C4–N2 1.381(7), C4–N3 1.303(7), C4–C5 1.480(8), C6–N3 1.434(7), Ir1–C1 2.004(6), Ir1–N3 2.111(4), Ir1–C26 2.202(6), Ir1–C27 2.189(6), Ir1–C30 2.140(5), Ir1–C31 2.113(6), C26–C27 1.38(1), C30–C31 1.39(1), Rh1–N1 2.079(5), Rh1–Cl1 2.371(2), Rh1–C18 2.091(6), Rh1–C19 2.113(6), Rh1–C22 2.134(6), Rh1–C23 2.127(6), C18–C19 1.407(9), C22–C23 1.38(1); N1-C1-N2 105.0(5), C1-Ir1-N3 78.4(2), C1-Ir1-C30 98.4(2), C1-Ir1-C31 95.0(2), N3-Ir1-C26 95.7(2), N3-Ir1-C27 99.7(2), N1-Rh1-Cl1 88.4 (2), N1-Rh1-C18 90.3(2), N1-Rh1-C19 91.2(2), Cl1-Rh1-C22 94.1(2), Cl1-Rh1-C23 90.5(3).

shown in Scheme 14 clearly indicate that the formation of the Ir–C bond represent a thermodynamic driving force.

A comparative ^{1}H NMR experiment was performed with either complex **1a** and 0.5 equivalent of [Rh(cod)(μ-Cl)]$_2$ or complex **1b** with 0.5 equivalent of [Ir(cod)(μ-Cl)]$_2$ in CD_2Cl_2 at room temperature, in the absence of KHMDS. A mixture of

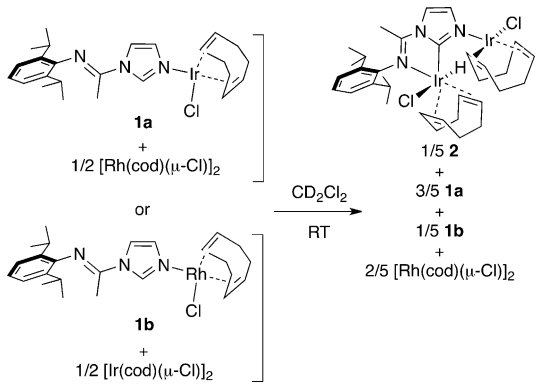

Scheme 15. The reactions between **1a** and $[Rh(cod)(\mu\text{-}Cl)]_2$, **1b** and $[Ir(cod)(\mu\text{-}Cl)]_2$ in the absence of KHMDS that were monitored by ^1H NMR spectroscopy.

complexes **1a**, **1b**, and **2** in a 3:1:1 ratio was obtained, indicating the occurrence of competing reactions (Scheme 15).

The reaction between complex **1a** and 0.5 equivalent of $[Rh(cod)(\mu\text{-}Cl)]_2$ could be viewed as a two-step process (Scheme 15), the first step would be a partial N-bound metal exchange, liberating some $[Ir(cod)(\mu\text{-}Cl)]_2$ that could react in a second step with complex **1a** to give complex **2** as a result of the C2–H bond activation. Starting from complex **1b** and $[Ir(cod)(\mu\text{-}Cl)]_2$ a metal exchange is thermodynamically favored and the resulting complex **1a** reacts then with $[Ir(cod)(\mu\text{-}Cl)]_2$ as described above. Somewhat surprisingly, a C2–H bond activation of complex **1b** by $[Ir(cod)(\mu\text{-}Cl)]_2$ to give a $\kappa^2(C2,N_{imine})Ir^{III},\kappa(N3)Rh^{I}$ complex was never observed.

Conclusion

A comparative study between Ir^I and Rh^I by using imine-functionalized imidazoles as potential precursors to functionalized pNHC complexes has revealed details of the mechanistic steps prior and during the C2–H metallation that leads to the pNHC complexes. In the case of iridium, the observation of Ir–H intermediates by ^1H NMR spectroscopy is consistent with the involvement of the (isolable) $N_{imidazole}$–Ir complex precursors undergoing tautomerization/metallotropism, followed by a chelate assisted C2–H bond activation in a neutral and a cationic intermediate. In the case of rhodium, C2-metallation proceeded only under forcing conditions at higher temperatures and intermediates analogous to those observed for Ir remained elusive. A new Rh^I–Ir^I heterodinuclear complex was obtained in a stepwise manner, which allowed the chemoselectivity of the synthetic approach to be investigated and understood. The $\kappa^2(C2,N_{imine})Ir^{I},\kappa(N3)Rh^{I}$ complex was selectively isolated, either starting from the N-bound Ir or from the N-bound Rh precursor. These results are in agreement with the preferred formation of strong, inert Ir–C bonds and can rationalize the carbophilic migration of the iridium (from complex **1a** to complex **12**, Scheme 14). It is anticipated that the results described above could be useful for the further development of synthetic methodologies to pNHC, C-bound "anionic" imidazolide, and relevant homo- and heterodinuclear complexes.

Experimental Section

General considerations: All manipulations involving organometallics were performed under argon in a Braun glovebox or by using standard Schlenk techniques. Solvents were dried by using standard methods and distilled over sodium/benzophenone under argon prior to use or passed through columns of activated alumina and subsequently purged with argon. $[Ir(cod)(\mu\text{-}Cl)]_2$ is commercially available from Johnson Matthey PLC. $[Rh(cod)(\mu\text{-}Cl)]_2$,[24] 1-(2,6-diisopropylphenylimino)ethylimidazole (H^{C2}**L**),[16f] 4(5)-carbethoxy-5(4)-methylimidazole,[25] *N*-(2,6-diisopropylphenyl)acetimidoyl chloride,[16f] complexes **1a**,[19] **2**,[19] **3a**$^+[PF_6]^-$,[19] and **4b**[20] were prepared according to the literature. NMR spectra of organic compounds and complexes were recorded on a Bruker 300, 400, or 500 MHz instrument at ambient temperature and referenced by using the proton (^1H) or carbon (^{13}C) resonance of the residual solvent. Assignments are based on ^1H,^1H-COSY, ^1H-NOESY, ^1H/^{13}C-HSQC, and ^1H/^{13}C-HMBC experiments. $^{31}P\{^1H\}$ NMR spectra were recorded on a Bruker Avance 300 instrument at 121.49 MHz by using H_3PO_4 (85% in D_2O) as external standard. IR spectra were recorded in the region $\tilde{\nu}=4000$–$100\ cm^{-1}$ on a Nicolet 6700 FT-IR spectrometer (ATR mode, diamond crystal). Elemental analyses were performed by the "Service de microanalyses" of the Université de Strasbourg.

Synthesis of 4(5)-methyl-5(4)-hydroxymethylimidazole: To a stirred suspension of 4(5)-carbethoxy-5(4)-methylimidazole (1.54 g, 10.00 mmol) in THF (100 mL) at 0 °C was added slowly lithium aluminium hydride (1.00 g, 26.35 mmol). The reaction mixture was heated to reflux for 4 h and then quenched by sequential addition of H_2O (1 mL), 15% aqueous NaOH solution (1 mL), and H_2O (3 mL) at 0 °C. After an appropriate amount of sodium sulfate was added to the mixture, it was further stirred for 30 min. The resultant solution was filtered through Celite and the filtrate was evaporated under reduced pressure to yield a white solid (1.00 g, 8.92 mmol, 89%).

Synthesis of 4(5)-methyl-5(4)-(2,6-di*iso*propylphenylimino) methylimidazole: To a stirred solution of 4(5)-methyl-5(4)-hydroxymethylimidazole (0.56 g, 5.00 mmol) in EtOH (50 mL) was added MnO_2 (0.87 g, 10.00 mmol). The reaction mixture was heated to reflux for 12 h. After filtration through Celite, 2,6-diisopropylaniline (0.89 g, 5.00 mmol) and a catalytic amount of 4-methylbenzenesulfonic acid were added to the filtrate. The reaction mixture was further heated to reflux for 6 h. After the solvent was evaporated under reduced pressure, the residue was washed with petroleum ether (3×3 mL) and dried under vacuum to give a white powder (0.68 g, 2.52 mmol, 50%). ^1H NMR (500 MHz, $CDCl_3$): $\delta=11.90$ (br s, 1H; N*H*), 8.13 (s, 1H; N=C*H*), 7.21–7.17 (m, 3H; $CH_{(Dipp)}$), 6.75 (br s, 1H; NC*H*NH), 3.00 (sept, $^3J=6.9$ Hz, 2H; C*H*$(CH_3)_2$), 2.36 (s, 3H; $CH_{3(imidazole)}$), 1.12 ppm (d, $^3J=6.9$ Hz, 12H; CH(CH_3)$_2$); $^{13}C\{^1H\}$ NMR (125 MHz, $CDCl_3$): $\delta=151.3$ (N=CH), 147.9 ($C_{(Dipp)}$), 144.2 (br s, $C_{(imidazole)}$), 138.8 ($C_{(Dipp)}$), 138.3 (NCHNH), 125.5 (br s, $C_{(imidazole)}$), 125.3 ($CH_{(Dipp)}$), 123.6 ($CH_{(Dipp)}$), 28.1 (*C*H$(CH_3)_2$), 23.7 (CH(CH_3)$_2$), 12.7 ppm ($CH_{3(imidazole)}$); IR (pure, orbit diamond): $\tilde{\nu}_{max}=1637\ cm^{-1}$ (ν(C=N)); elemental analysis calcd for $C_{17}H_{23}N_3$ (269.39): C 75.80, H 8.61, N 15.60; found: C 75.41, H 8.64, N 15.93.

Synthesis of 1-(2,6-diisopropylphenylimino)ethyl-4-(2,6-diisopropylphenylimino)methyl-5-methylimidazole (H^{C2}L′): To a stirred solution of 4(5)-methyl-5(4)-(2,6-diisopropylphenylimino) methylimidazole (1.00 g, 3.71 mmol) and triethylamine (1.0 mL, 7.17 mmol) in CH_2Cl_2 (10 mL) was added *N*-(2,6-diisopropylphenyl) acetimidoyl chloride (0.88 g, 3.71 mmol). The reaction mixture was stirred for 12 h at room temperature. After removal of the volatiles under reduced pressure, the residue was extracted with Et_2O and the solu-

tion was filtered through Celite. The filtrate was evaporated under reduced pressure. Then the residue was washed with pentane (3× 1 mL) and dried under vacuum to give a yellow powder (1.57 g, 3.34 mmol, 90%). ^{1}H NMR (500 MHz, $CDCl_3$): $\delta = 8.68$ (s, 1H; N=CH), 8.00 (s, 1H; $NCHN_{(near\ imine)}$), 7.23–7.00 (m, 6H; $CH_{(Dipp)}$), 3.00 (sept, $^3J = 6.9$ Hz, 2H; $CH(CH_3)_2$), 2.79 (sept, $^3J = 6.9$ Hz, 2H; $CH(CH_3)_2$), 2.61 (s, 3H; $CH_{3(imidazole)}$), 2.28 (s, 3H; $CH_{3(imine)}$), 1.12 (d, $^3J = 6.9$ Hz, 18H; $CH(CH_3)_2$), 1.05 ppm (d, $^3J = 6.9$ Hz, 6H; $CH(CH_3)_2$); ^{13}C{^{1}H} NMR (125 MHz, $CDCl_3$): $\delta = 153.2$ (N=CH), 152.3 ($N=CCH_3$), 149.9 ($C_{(Dipp)}$), 146.9 ($C_{(imidazole)}$), 142.5 ($C_{(Dipp)}$), 137.9 ($NCHN_{(near\ imine)}$), 137.7 ($C_{(Dipp)}$), 136.8 ($C_{(Dipp)}$), 125.2 ($C_{(imidazole)}$), 124.7 ($CH_{(Dipp)}$), 124.1 ($CH_{(Dipp)}$), 123.4 ($CH_{(Dipp)}$), 123.0 ($CH_{(Dipp)}$), 28.4 ($CH(CH_3)_2$), 27.9 ($CH(CH_3)_2$), 23.7 ($CH(CH_3)_2$), 23.5 ($CH(CH_3)_2$), 23.2 ($CH(CH_3)_2$), 19.1 ($CH_{3(imine)}$), 15.0 ($CH_{3(imidazole)}$); IR (pure, orbit diamond): $\tilde{\nu}_{max} = 1670$ cm^{-1} (ν(C=N)); elemental analysis calcd for $C_{31}H_{42}N_4$ (470.71): C 79.10, H 8.99, N 11.90; found: C 78.67, H 8.94, N 12.33.

Synthesis of [Rh(cod)Cl($H^{C2}L^{N3}$)] (1b); A solution of the ligand H^{C2}**L** (0.054 g, 0.20 mmol) in THF (2 mL) was added to a stirred solution of $[Rh(cod)(\mu\text{-}Cl)]_2$ (0.050 g, 0.10 mmol) in THF (3 mL). The reaction mixture was stirred for 1 h at room temperature and then the solvent was removed under reduced pressure. The residue was washed with pentane (3×1 mL) and dried under vacuum to give a yellow solid (0.093 g, 0.18 mmol, 90%). Single crystals of complex **1b** suitable for X-ray diffraction were obtained by slow evaporation of a saturated solution of complex **1b** in Et_2O at ambient temperature. ^{1}H NMR (500 MHz, CD_2Cl_2): $\delta = 8.72$ (s, 1H; $NCHN_{(near\ imine)}$), 7.80 (apparent t, $^{3,4}J = 1.5$ Hz, 1H; $NCHCHN_{(near\ imine)}$), 7.20–7.09 (m, 3H; $CH_{(Dipp)}$), 6.95 (apparent t, $^{3,4}J = 1.5$ Hz, 1H; $NCHCHN_{(near\ imine)}$), 4.80–3.70 (an overlap of two br s, 4H; $CH_{(cod)}$), 2.68 (sept, $^3J = 6.9$ Hz, 2H; $CH(CH_3)_2$), 2.56–2.40 (m, 4H; $CH_{2(cod)}$), 2.17 (s, 3H; $CH_{3(imine)}$), 1.93–1.77 (m, 4H; $CH_{2(cod)}$), 1.14 (d, $^3J = 6.9$ Hz, 6H; $CH(CH_3)_2$), 1.10 ppm (d, $^3J = 6.9$ Hz, 6H; $CH(CH_3)_2$); ^{13}C{^{1}H} NMR (125 MHz, CD_2Cl_2): $\delta = 149.0$ (C=N), 142.2 (*ipso*-$C_{(Dipp)}$), 138.6 ($NCHN_{(near\ imine)}$), 137.2 (*o*-$C_{(Dipp)}$), 127.9 ($NCHCHN_{(near\ imine)}$), 125.0 (*p*-$CH_{(Dipp)}$), 123.7 (*m*-$CH_{(Dipp)}$), 117.0 ($NCHCHN_{(near\ imine)}$), 83.0 (br, $CH_{(cod)}$), 76.2 (br, $CH_{(cod)}$), 31.2 (br, $CH_{2(cod)}$), 28.7 ($CH(CH_3)_2$), 23.3 ($CH(CH_3)_2$), 23.0 ($CH(CH_3)_2$), 16.4 ppm ($CH_{3(imine)}$). IR (pure, orbit diamond): $\tilde{\nu}_{max} = 1687$ (ν(C=N)), 280 cm^{-1} (ν(Rh–Cl)); elemental analysis calcd for $C_{25}H_{35}ClN_3Rh$ (515.92): C 58.20, H 6.84, N 8.14; found: C 58.18, H 6.77, N 8.27.

Synthesis of [Rh(cod)($H^{N3}L^{C2,Nimine}$)]$^+$[PF_6]$^-$ (3b$^+$[PF_6]$^-$) and [Rh(cod)($H^{C2}L^{N3}$)$_2$]$^+$[PF_6]$^-$ (6b$^+$[PF_6]$^-$): To a stirred solution of complex **1b** (0.103 g, 0.20 mmol) in CH_2Cl_2 (5 mL) was added $TlPF_6$ (0.070 g, 0.20 mmol). The reaction mixture was stirred for 12 h at room temperature. After filtration through Celite, the filtrate was concentrated under reduced pressure to approximately 2 mL and then the residue was stratified with Et_2O to yield **3b**$^+$[PF_6]$^-$ as dark red crystals, which were collected by filtration and dried in vacuo (0.005 g, 0.008 mmol, 4%). ^{1}H NMR (500 MHz, CD_2Cl_2): $\delta = 10.31$ (br s, 1H; NH), 7.36–7.25 (m, 4H; $NHCHCHN_{(near\ imine)}$, $CH_{(Dipp)}$), 7.23 (apparent t, $^3J = 2.3$ Hz, 1H; $NHCHCHN_{(near\ imine)}$), 4.68–4.60 (m, 2H; $CH_{(cod)}$), 4.27–4.19 (m, 2H; $CH_{(cod)}$), 3.10 (sept, $^3J = 6.8$ Hz, 2H; $CH(CH_3)_2$), 2.44–2.32 (m, 5H; $CH_{2(cod)}$, $CH_{3(imine)}$), 2.29–2.17 (m, 4H; $CH_{2(cod)}$), 2.12–2.00 (m, 2H; $CH_{2(cod)}$), 1.37 (d, $^3J = 6.8$ Hz, 6H; $CH(CH_3)_2$), 1.13 ppm (d, $^3J = 6.8$ Hz, 6H; $CH(CH_3)_2$); ^{13}C{^{1}H} NMR (125 MHz, CD_2Cl_2): $\delta = 176.9$ (d, ^1J(Rh,C) = 55.1 Hz, $NHCN_{(near\ imine)}$), 163.7 (C=N), 140.6 (*o*-$C_{(Dipp)}$), 138.7 (*ipso*-$C_{(Dipp)}$), 128.5 (*p*-$CH_{(Dipp)}$), 124.9 (*m*-$CH_{(Dipp)}$), 121.4 ($NHCHCHN_{(near\ imine)}$), 116.1 ($NHCHCHN_{(near\ imine)}$), 105.6 (d, ^1J(Rh,C) = 6.8 Hz, $CH_{(cod)}$), 78.9 (d, ^1J(Rh,C) = 12.6 Hz, $CH_{(cod)}$), 32.0 ($CH_{2(cod)}$), 29.0 ($CH_{2(cod)}$), 28.9 ($CH(CH_3)_2$), 25.0 ($CH(CH_3)_2$), 23.3 ($CH(CH_3)_2$), 16.3 ppm ($CH_{3(imine)}$); ^{31}P{^{1}H} NMR (121.5 MHz, CD_2Cl_2): $\delta = -144.1$ ppm (sept, ^1J(P,F) = 712 Hz, PF_6^-); ^{19}F{^{1}H} NMR (282.4 MHz, CD_2Cl_2): $\delta = -73.5$ ppm (d, ^1J(P,F) = 712 Hz, PF_6^-); IR (pure, orbit diamond): $\tilde{\nu}_{max} = 3405$ (ν(N–H)), 1627 (ν(C=N)), 827 cm^{-1} (ν(P–F)); elemental analysis calcd for $C_{25}H_{35}F_6RhN_3P$ (625.45): C 48.01, H 5.64, N 6.72; found: C 47.92, H 5.65, N 6.71.

The above-described filtrate was further concentrated under reduced pressure to approximately 2 mL. A yellow precipitate was formed after pentane (5 mL) was added to the solution. The precipitate was filtered, washed with pentane (2×3 mL) and dried under vacuum to give complex **6b**$^+$[PF_6]$^-$ as a pale yellow powder (0.081 g, 0.090 mmol, 90% (based on **L**)). ^{1}H NMR (500 MHz, CD_2Cl_2): $\delta = 8.42$ (br s, 2H; $NCHN_{(near\ imine)}$), 7.80 (s, 2H; $NCHCHN_{(near\ imine)}$), 7.23–7.09 (m, 6H; $CH_{(Dipp)}$), 7.04 (s, 2H; $NCHCHN_{(near\ imine)}$), 4.24 (br s, 4H; $CH_{(cod)}$), 2.67 (sept, $^3J = 6.7$ Hz, 4H; $CH(CH_3)_2$), 2.62–2.52 (m, 4H; $CH_{2(cod)}$), 2.19 (s, 6H; $CH_{3(imine)}$), 2.02–1.86 (m, 4H; $CH_{2(cod)}$), 1.14 (d, $^3J = 6.7$ Hz, 12H; $CH(CH_3)_2$), 1.09 ppm (d, $^3J = 6.7$ Hz, 12H; $CH(CH_3)_2$); ^{13}C{^{1}H} NMR (125 MHz, CD_2Cl_2): $\delta = 149.2$ (C=N), 142.2 (*ipso*-$C_{(Dipp)}$), 137.2 (*o*-$C_{(Dipp)}$), 137.0 ($NCHN_{(near\ imine)}$), 129.0 ($NCHCHN_{(near\ imine)}$), 125.1 (*p*-$CH_{(Dipp)}$), 123.7 (*m*-$CH_{(Dipp)}$), 117.6 ($NCHCHN_{(near\ imine)}$), 83.8 (br, $CH_{(cod)}$), 31.1 ($CH_{2(cod)}$), 28.7 ($CH(CH_3)_2$), 23.3 ($CH(CH_3)_2$), 22.9 ($CH(CH_3)_2$), 16.3 ppm ($CH_{3(imine)}$); ^{31}P{^{1}H} NMR (121.5 MHz, CD_2Cl_2): $\delta = -144.3$ ppm (sept, ^1J(P,F) = 712 Hz, PF_6^-); ^{19}F{^{1}H} NMR (282.4 MHz, CD_2Cl_2): $\delta = -73.4$ ppm (d, ^1J(P,F) = 712 Hz, PF_6^-); IR (pure, orbit diamond): $\tilde{\nu}_{max} = 1685$ (ν(C=N)), 840 cm^{-1} (ν(P–F)); elemental analysis calcd for $C_{42}H_{58}F_6N_6PRh$ (894.84): C 56.37, H 6.53, N 9.39; found: C 56.90, H 6.75, N 9.74.

Improved synthesis of [Rh(cod)($H^{N3}L^{C2,Nimine}$)]$^+$[PF_6]$^-$ (3b$^+$[PF_6]$^-$): To a stirred solution of complex **1b** (0.044 g, 0.086 mmol) in toluene (2 mL) was added $TlPF_6$ (0.030 g, 0.086 mmol). The reaction mixture was stirred for 12 h at 110 °C. The resulting red precipitate was collected by filtration and dissolved in CH_2Cl_2 (3 mL). After filtration through Celite, the filtrate was evaporated under reduced pressure to yield a dark red crystalline solid (0.048 g, 0.077 mmol, 90%).

Synthesis of [Ir(cod)Cl{$C_3H_3N_2$(*n*Bu)-κN3}] (4a): A solution of 1-*n*-butylimidazole (0.019 g, 0.15 mmol) in THF (2 mL) was added to a stirred solution of $[Ir(cod)(\mu\text{-}Cl)]_2$ (0.050 g, 0.074 mmol) in THF (3 mL). The reaction mixture was stirred for 1 h at room temperature and then the solvent was removed in vacuo. The residue was washed with pentane (3×1 mL) and dried under vacuum to give a yellow solid (0.062 g, 0.13 mmol, 90%). ^{1}H NMR (500 MHz, CD_2Cl_2): $\delta = 8.08$ (br s, 1H; $NCHN_{(nBu)}$), 7.01 (s, 1H; $NCHCHN_{(nBu)}$), 6.96 (s, 1H; $NCHCHN_{(nBu)}$), 3.94 (t, $^3J = 7.4$ Hz, 2H; $NCH_2CH_2CH_2CH_3$), 3.89 (br s, 4H; $CH_{(cod)}$), 2.30–2.14 (m, 4H; $CH_{2(cod)}$), 1.75 (quint, $^3J = 7.4$ Hz, 2H; $NCH_2CH_2CH_2CH_3$), 1.62–1.46 (m, 4H; $CH_{2(cod)}$), 1.31 (sext, $^3J = 7.4$ Hz, 2H; $NCH_2CH_2CH_2CH_3$), 0.92 ppm (t, $^3J = 7.4$ Hz, 3H; $NCH_2CH_2CH_2CH_3$); ^{13}C{^{1}H} NMR (125 MHz, CD_2Cl_2): $\delta = 139.1$ ($NCHN_{(nBu)}$), 127.2 ($NCHCHN_{(nBu)}$), 119.8 ($NCHCHN_{(nBu)}$), 62.5 (br, $CH_{(cod)}$), 48.1 ($NCH_2CH_2CH_2CH_3$), 33.0 ($NCH_2CH_2CH_2CH_3$), 31.8 ($CH_{2(cod)}$), 20.0 ($NCH_2CH_2CH_2CH_3$), 13.6 ppm ($NCH_2CH_2CH_2CH_3$); elemental analysis calcd for $C_{15}H_{24}ClIrN_2$ (460.04): C 39.16, H 5.26, N 6.09; found: C 38.64, H 5.43, N 6.55.

Synthesis of [Ir(cod){$C_3H_3N_2$(*n*Bu)-κN3}$_2$]$^+$[PF_6]$^-$ (5a$^+$[PF_6]$^-$): To a stirred solution of complex **4a** (0.046 g, 0.10 mmol) in CH_2Cl_2 (5 mL) was added $TlPF_6$ (0.035 g, 0.10 mmol). The reaction mixture was stirred for 12 h at room temperature. After filtration through Celite, the filtrate was evaporated to dryness under reduced pressure. The residue was washed with Et_2O (3×1 mL) and dried under vacuum to give a yellow solid (0.028 g, 0.041 mmol, 82%). ^{1}H NMR (500 MHz, CD_2Cl_2): $\delta = 7.42$ (s, 2H; $NCHN_{(nBu)}$), 7.07 (s, 2H; $NCHCHN_{(nBu)}$), 6.81 (s, 2H; $NCHCHN_{(nBu)}$), 3.99 (t, $^3J = 7.4$ Hz, 4H; $NCH_2CH_2CH_2CH_3$), 3.83 (br s, 4H; $CH_{(cod)}$), 2.38–2.28 (m, 4H; $CH_{2(cod)}$), 1.82–1.66 (m, 8H; $NCH_2CH_2CH_2CH_3$, $CH_{2(cod)}$), 1.27 (sext, $^3J = 7.4$ Hz, 4H; $NCH_2CH_2CH_2CH_3$), 0.91 ppm (t, $^3J = 7.4$ Hz, 6H; $NCH_2CH_2CH_2CH_3$); ^{13}C{^{1}H} NMR (125 MHz, CD_2Cl_2): $\delta = 138.0$

($NCHN_{(nBu)}$), 127.9 ($NCHCHN_{(nBu)}$), 121.2 ($NCHCHN_{(nBu)}$), 67.2 ($CH_{(cod)}$), 48.6 ($NCH_2CH_2CH_2CH_3$), 32.7 ($NCH_2CH_2CH_2CH_3$), 31.6 ($CH_{2(cod)}$), 19.9 ($NCH_2CH_2CH_2CH_3$), 13.6 ppm ($NCH_2CH_2CH_2CH_3$); $^{31}P\{^1H\}$ NMR (121.5 MHz, CD_2Cl_2): $\delta = -144.4$ ppm (sept, $^1J(P,F) = 712$ Hz, PF_6^-); $^{19}F\{^1H\}$ NMR (282.4 MHz, CD_2Cl_2): $\delta = -73.4$ (d, $^1J(P,F) = 712$ Hz, PF_6^-); elemental analysis calcd for $C_{22}H_{36}F_6IrN_4P$ (693.74): C 38.09, H 5.23, N 8.08; found: C 37.61, H 5.70, N 8.55.

Synthesis of $[Ir(cod)\{C_3H_3N_2(Mes)$-κN3$\}_2]^+[PF_6]^-$ ($5b^+[PF_6]^-$): To a stirred solution of complex **4b** (0.052 g, 0.10 mmol) in CH_2Cl_2 (5 mL) was added $TlPF_6$ (0.035 g, 0.10 mmol). The reaction mixture was stirred for 12 h at room temperature. After filtration through Celite, the filtrate was evaporated to dryness under reduced pressure. The residue was washed with Et_2O (3×1 mL) and dried under vacuum to give a yellow solid (0.038 g, 0.046 mmol, 92%). ^1H NMR (500 MHz, CD_2Cl_2): $\delta = 7.52$ (apparent t, $^4J = 1.3$ Hz, 2H; $NCHN_{(Mes)}$), 7.11 (apparent t, $^{3,4}J = 1.3$ Hz, 1H; $NCHCHN_{(Mes)}$), 7.07 (apparent t, $^{3,4}J = 1.3$ Hz, 2H; $NCHCHN_{(Mes)}$), 7.02 (s, 4H; *m*-$CH_{(Mes)}$), 3.97–3.89 (m, 4H; $CH_{(cod)}$), 2.43–2.35 (m, 4H; $CH_{2(cod)}$), 2.34 (s, 6H; *p*-$CH_{3(Mes)}$), 1.92 (s, 12H; *o*-$CH_{3(Mes)}$), 1.85–1.77 ppm (m, 4H; $CH_{2(cod)}$); $^{13}C\{^1H\}$ NMR (125 MHz, CD_2Cl_2): $\delta = 141.0$ (*p*-$C_{(Mes)}$), 138.4 ($NCHN_{(Mes)}$), 134.9 (*o*-$C_{(Mes)}$), 131.9 (*ipso*-$C_{(Mes)}$), 129.8 (*m*-$CH_{(Mes)}$), 128.5 ($NCHCHN_{(Mes)}$), 123.1 ($NCHCHN_{(Mes)}$), 68.2 ($CH_{(cod)}$), 31.7 ($CH_{2(cod)}$), 21.2 (*p*-$CH_{3(Mes)}$), 17.4 ppm (*o*-$CH_{3(Mes)}$); $^{31}P\{^1H\}$ NMR (121.5 MHz, CD_2Cl_2): $\delta = -144.5$ ppm (sept, $^1J(P,F) = 712$ Hz, PF_6^-); $^{19}F\{^1H\}$ NMR (282.4 MHz, CD_2Cl_2): $\delta = -73.4$ ppm (d, $^1J(P,F) = 712$ Hz, PF_6^-); elemental analysis calcd for $C_{32}H_{40}F_6IrN_4P$ (817.88): C 46.99, H 4.93, N 6.85; found: C 47.07, H 4.60, N 7.24.

Synthesis of $[Ir(cod)(H^{C2}L^{N3})_2]^+[PF_6]^-$ ($6a^+[PF_6]^-$): To a stirred solution of complex **1a** (0.030 g, 0.050 mmol) and $H^{C2}L$ (0.014 g, 0.052 mmol) in CH_2Cl_2 (2 mL) was added $TlPF_6$ (0.018 g, 0.052 mmol). The reaction mixture was stirred for 2 h at room temperature. After filtration through Celite, the filtrate was evaporated to dryness under reduced pressure. The residue was washed with Et_2O (3×1 mL) and dried under vacuum to give a yellow powder (0.045 g, 0.046 mmol, 92%). Single crystals of complex $\mathbf{6a}^+[PF_6]^-$ suitable for X-ray diffraction were obtained by slow evaporation of a saturated solution in Et_2O at ambient temperature. ^1H NMR (500 MHz, CD_2Cl_2): $\delta = 8.41$ (s, 2H; $NCHN_{(near\ imine)}$), 7.91 (s, 2H; $NCHCHN_{(near\ imine)}$), 7.20–7.07 (m, 8H; $CH_{(Dipp)}$, $NCHCHN_{(near\ imine)}$), 3.98 (brs, 4H; $CH_{(cod)}$), 2.67 (sept, $^3J = 6.9$ Hz, 4H; $CH(CH_3)_2$), 2.51–2.35 (m, 4H; $CH_{2(cod)}$), 2.22 (s, 6H; $CH_{3(imine)}$), 1.91–1.75 (m, 4H; $CH_{2(cod)}$), 1.14 (d, $^3J = 6.9$ Hz, 12H; $CH(CH_3)_2$), 1.08 ppm (d, $^3J = 6.9$ Hz, 12H; $CH(CH_3)_2$); $^{13}C\{^1H\}$ NMR (125 MHz, CD_2Cl_2): $\delta = 149.2$ (C=N), 141.9 (*ipso*-$C_{(Dipp)}$), 137.1 (*o*-$C_{(Dipp)}$), 136.7 ($NCHN_{(near\ imine)}$), 129.0 ($NCHCHN_{(near\ imine)}$), 125.3 (*p*-$CH_{(Dipp)}$), 123.7 (*m*-$CH_{(Dipp)}$), 118.4 ($NCHCHN_{(near\ imine)}$), 68.9 ($CH_{(cod)}$), 31.7 ($CH_{2(cod)}$), 28.7 ($CH(CH_3)_2$), 23.4 ($CH(CH_3)_2$), 22.9 ($CH(CH_3)_2$), 16.2 ppm ($CH_{3(imine)}$); $^{31}P\{^1H\}$ NMR (121.5 MHz, CD_2Cl_2): δ0−144.4 ppm (sept, $^1J(P,F) = 712$ Hz, PF_6^-); $^{19}F\{^1H\}$ NMR (282.4 MHz, CD_2Cl_2): $\delta = -73.4$ ppm (d, $^1J(P,F) = 712$ Hz, PF_6^-); IR (pure, orbit diamond): $\tilde{\nu}_{max} = 1687$ (ν(C=N)), 833 cm^{-1} (ν(P–F)); elemental analysis calcd for $C_{42}H_{58}F_6N_6PIr$ (984.15): C 51.26, H 5.94, N 8.54; found: C 50.81, H 5.93, N 8.44.

Synthesis of $[Ir(cod)(PPh_3)(H^{N3}L^{C2,Nimine})]^+[PF_6]^-$ ($7a^+[PF_6]^-$): To a stirred solution of complex $\mathbf{3a}^+[PF_6]^-$ (0.040 g, 0.056 mmol) in CH_2Cl_2 (3 mL) was added a solution of PPh_3 (0.015 g, 0.057 mmol) in CH_2Cl_2 (2 mL). The reaction mixture was stirred for 1 h at room temperature. After the solution was concentrated under reduced pressure to approximately 2 mL, the solution was stratified with Et_2O to yield after diffusion green crystals, which were collected by filtration and dried in vacuo (0.046 g, 0.047 mmol, 84%). ^1H NMR (500 MHz, CD_2Cl_2): $\delta = 9.69$ (brs, 1H; NH), 7.53–7.26 (m, 12H; $CH_{(Ar)}$), 7.22 (apparent t, $^3J = 2.3$ Hz, 1H; $NHCHCHN_{(near\ imine)}$), 7.06 (brs, 6H; $CH_{(Ar)}$), 6.99 (apparent t, $^3J = 2.3$ Hz, 1H; $NHCHCHN_{(near\ imine)}$), 5.10–4.00 (brs, 2H; $CH_{(cod)}$), 4.00–3.20 (brs, 2H; $CH_{(cod)}$), 2.75 (brs„ 2H; $CH(CH_3)_2$), 2.37 (s, 3H; $CH_{3(imine)}$), 1.89 (brs, 4H; $CH_{2(cod)}$), 1.71 (brs, 4H; $CH_{2(cod)}$), 1.48–0.56 ppm (m, 12H; $CH(CH_3)_2$); $^{13}C\{^1H\}$ NMR (125 MHz, CD_2Cl_2): $\delta = 173.8$ ($NHCN_{(near\ imine)}$), 158.7 (br, C=N), 141.7 ($C_{(Dipp)}$), 141.2 (br, $C_{(Dipp)}$), 134.7 (d, $^1J(P,C) = 39.4$ Hz, *ipso*-$C_{(PPh_3)}$), 133.1 (d, $J(P,C) = 5.3$ Hz, $CH_{(PPh_3)}$), 130.5 ($CH_{(PPh_3)}$), 129.2 (d, $J(P,C) = 9.1$ Hz, $CH_{(PPh_3)}$), 127.9 ($CH_{(Dipp)}$), 125.0 (br, $CH_{(Dipp)}$), 122.0 ($NHCHCHN_{(near\ imine)}$), 117.0 ($NHCHCHN_{(near\ imine)}$), 88.7 (br, $CH_{(cod)}$), 30.1 ($CH_{2(cod)}$), 28.4 (br, $CH(CH_3)_2$), 25.3 ($CH(CH_3)_2$), 24.2 (br, $CH(CH_3)_2$), 19.3 ppm ($CH_{3(imine)}$); $^{31}P\{^1H\}$ NMR (121.5 MHz, CD_2Cl_2): $\delta = -1.9$ (s, PPh_3), −144.1 ppm (sept, $^1J(P,F) = 712$ Hz, PF_6^-); $^{19}F\{^1H\}$ NMR (282.4 MHz, CD_2Cl_2): $\delta = -73.5$ ppm (d, $^1J(P,F) = 712$ Hz, PF_6^-); IR (pure, orbit diamond): $\tilde{\nu}_{max} = 3390$ (ν(N–H)), 1617 (ν(C=N)), 839 cm^{-1} (ν(P–F)); elemental analysis calcd for $C_{43}H_{50}F_6IrN_3P_2$ (977.05): C 52.86, H 5.16, N 4.30; found: C 52.39, H 5.33, N 4.14.

Synthesis of $[Ir(cod)(PMe_3)(H^{N3}L^{C2,Nimine})]^+[PF_6]^-$ ($7b^+[PF_6]^-$): To a stirred solution of complex $\mathbf{3a}^+[PF_6]^-$ (0.040 g, 0.056 mmol) in CH_2Cl_2 (3 mL) was added a solution of PMe_3 (0.1 M in Et_2O, 0.60 mL, 0.060 mmol). The reaction mixture was stirred for 1 h at room temperature. After removal of the volatiles under reduced pressure, the residue was washed with Et_2O (3×1 mL) to yield a yellow powder, which was collected by filtration and dried in vacuo (0.038 g, 0.048 mmol, 86%). ^1H NMR (500 MHz, CD_2Cl_2): $\delta = 10.08$ (brs, 1H; NH), 7.47 (apparent t, $J = 2.4$ Hz, 1H; $NHCHCHN_{(near\ imine)}$), 7.36 (apparent t, $^3J = 2.4$ Hz, 1H; $NHCHCHN_{(near\ imine)}$), 7.35–7.21 (m, 3H; $CH_{(Dipp)}$), 4.00–3.86 (m, 1H; $CH_{(cod)}$), 3.64–3.48 (m, 2H; $CH_{(cod)}$), 2.86–2.78 (m, 1H; $CH_{(cod)}$), 2.72 (sept, $^3J = 6.7$ Hz, 1H; $CH(CH_3)_2$), 2.58 (sept, $^3J = 6.7$ Hz, 1H; $CH(CH_3)_2$), 2.52–2.38 (m, 2H; $CH_{2(cod)}$), 2.26 (d, $^5J(H,P) = 4.3$ Hz, 3H; $CH_{3(imine)}$), 2.20–1.94 (m, 3H; $CH_{2(cod)}$), 1.46–1.32 (m, 3H; $CH_{2(cod)}$), 1.30 (d, $^3J = 6.7$ Hz, 3H; $CH(CH_3)_2$), 1.26–1.20 (m, 12H; $P(CH_3)_3$, $CH(CH_3)_2$), 1.09 (d, $^3J = 6.7$ Hz, 3H; $CH(CH_3)_2$), 1.02 ppm (d, $^3J = 6.7$ Hz, 3H; $CH(CH_3)_2$); $^{13}C\{^1H\}$ NMR (125 MHz, CD_2Cl_2): $\delta = 171.1$ (d, $^2J(P,C) = 10.9$ Hz, $NHCN_{(near\ imine)}$), 155.3 (d, $^3J(P,C) = 6.2$ Hz, C=N), 142.6 ($C_{(Dipp)}$), 140.9 ($C_{(Dipp)}$), 140.2 ($C_{(Dipp)}$), 128.1 ($CH_{(Dipp)}$), 125.5 ($CH_{(Dipp)}$), 124.5 ($CH_{(Dipp)}$), 121.8 ($NHCHCHN_{(near\ imine)}$), 115.3 ($NHCHCHN_{(near\ imine)}$), 94.4 (d, $^2J(P,C) = 4.6$ Hz, $CH_{(cod)}$), 73.4 ($CH_{(cod)}$), 58.2 (d, $^2J(P,C) = 16.6$ Hz, $CH_{(cod)}$), 42.0 ($CH_{2(cod)}$), 41.1 (d, $^2J(P,C) = 2.3$ Hz, $CH_{(cod)}$), 33.3 ($CH_{2(cod)}$), 30.0 ($CH_{2(cod)}$), 29.5 ($CH_{2(cod)}$), 27.8 (d, $^5J(P,C) = 3.9$ Hz, $CH(CH_3)_2$), 27.5 ($CH(CH_3)_2$), 24.8 ($CH(CH_3)_2$), 24.7 ($CH(CH_3)_2$), 24.4 ($CH(CH_3)_2$), 24.2 ($CH(CH_3)_2$), 17.5 ($CH_{3(imine)}$), 16.1 ppm (d, $^1J(P,C) = 28.1$ Hz, PCH_3); $^{31}P\{^1H\}$ NMR (121.5 MHz, CD_2Cl_2): $\delta = -44.8$ (s, $P(CH_3)_3$), −144.3 ppm (sept, $^1J(P,F) = 712$ Hz, PF_6^-); $^{19}F\{^1H\}$ NMR (282.4 MHz, CD_2Cl_2): $\delta = -73.5$ ppm (d, $^1J(P,F) = 712$ Hz, PF_6^-). IR (pure, orbit diamond): $\tilde{\nu}_{max} = 3381$ (ν(N–H)), 1608 (ν(C=N)), 835 cm^{-1} (ν(P–F)); elemental analysis calcd for $C_{28}H_{44}F_6IrN_3P_2$ (790.84): C 42.53, H 5.61, N 5.31; found: C 42.32, H 5.71, N 5.11.

Synthesis of $[Ir(cod)Cl(H^{C2}L'^{N3})]$ (8): A solution of $H^{C2}L'$ (0.071 g, 0.15 mmol) in THF (2 mL) was added to a stirred solution of $[Ir(cod)(\mu\text{-}Cl)]_2$ (0.050 g, 0.074 mmol) in THF (3 mL). The reaction mixture was stirred for 1 h at room temperature and then the solvent was removed under reduced pressure. The residue was washed with pentane (3×1 mL) and dried under vacuum to give a yellow solid (0.103 g, 0.13 mmol, 85%). ^1H NMR (500 MHz, CD_2Cl_2): $\delta = 8.70$ (s, 1H; N=CH), 8.19 (s, 1H; $NCHN_{(near\ imine)}$), 7.20–7.00 (m, 6H; $CH_{(Dipp)}$), 4.42–4.34 (m, 2H; $CH_{(cod)}$), 3.38–3.30 (m, 2H; $CH_{(cod)}$), 3.00–2.92 (m, 5H; $CH(CH_3)_2$, $CH_{3(imidazole)}$), 2.69 (sept, $^3J = 6.9$ Hz, 2H; $CH(CH_3)_2$), 2.37–2.29 (m, 4H; $CH_{2(cod)}$), 2.28 (s, 3H; $CH_{3(imine)}$), 1.72–1.48 (m, 4H; $CH_{2(cod)}$), 1.11 (d, $^3J = 6.9$ Hz, 6H; $CH(CH_3)_2$), 1.09 (d, $^3J = 6.9$ Hz, 12H; $CH(CH_3)_2$), 0.98 ppm (d, $^3J = 6.9$ Hz, 6H; $CH(CH_3)_2$); $^{13}C\{^1H\}$ NMR (125 MHz, CD_2Cl_2): $\delta = 153.5$ (N=CH), 151.6 (N=CCH_3), 149.6 ($C_{(Dipp)}$), 144.5 ($C_{(imidazole)}$), 142.0 ($C_{(Dipp)}$), 137.8 ($C_{(Dipp)}$), 136.9 ($C_{(Dipp)}$), 136.7 ($NCHN_{(near\ imine)}$), 126.4 ($C_{(imidazole)}$),

125.3 ($CH_{(Dipp)}$), 124.7 ($CH_{(Dipp)}$), 123.8 ($CH_{(Dipp)}$), 123.2 ($CH_{(Dipp)}$), 70.1 ($CH_{(cod)}$), 58.5 ($CH_{(cod)}$), 32.8 ($CH_{2(cod)}$), 31.5 ($CH_{2(cod)}$), 28.6 ($CH(CH_3)_2$), 28.1 ($CH(CH_3)_2$), 23.7 ($CH(CH_3)_2$), 23.2 ($CH(CH_3)_2$), 23.2 ($CH(CH_3)_2$), 18.8 ($CH_{3(imine)}$), 16.0 ppm ($CH_{3(imidazole)}$); IR (pure, orbit diamond): $\tilde{\nu}_{max}=1684\ cm^{-1}$ (ν(C=N)); elemental analysis calcd for $C_{39}H_{54}ClIrN_4$ (806.56): C 58.08, H 6.75, N 6.95; found: C 58.29, H 6.39, N 6.58.

Synthesis of $[Ir(cod)(H^{C2}L'^{N3,Nimine})]^+[PF_6]^-$ ($9^+[PF_6]^-$): $TlPF_6$ (0.035 g, 0.10 mmol) was added to a stirred solution of complex **8** (0.081 g, 0.10 mmol) in CH_2Cl_2 (5 mL). The reaction mixture was further stirred for 2 h at room temperature. After filtration through Celite, the filtrate was evaporated under reduced pressure. Then the residue was washed with pentane (3×1 mL) and dried under vacuum to give a dark red crystalline solid (0.080 g, 0.087 mmol, 87%). Single crystals of complex $\mathbf{9}^+[PF_6]^-$ suitable for X-ray diffraction were obtained by slow diffusion of a layer of pentane into a solution of complex $\mathbf{9}^+[PF_6]^-$ in THF at ambient temperature under argon. ^1H NMR (500 MHz, CD_2Cl_2): $\delta=8.30$ (s, 2H; N=CH, $NCHN_{(near\ imine)}$), 7.36–7.12 (m, 6H; $CH_{(Dipp)}$), 4.88–4.80 (m, 2H; $CH_{(cod)}$), 3.35–3.27 (m, 2H; $CH_{(cod)}$), 3.22 (sept, $^3J=6.9$ Hz, 2H; $CH(CH_3)_2$), 2.87 (s, 3H; $CH_{3(imidazole)}$), 2.69 (sept, $^3J=6.9$ Hz, 2H; $CH(CH_3)_2$), 2.36 (s, 3H; $CH_{3(imine)}$), 2.33–2.25 (m, 2H; $CH_{2(cod)}$), 2.25–2.17 (m, 2H; $CH_{2(cod)}$), 1.95–1.87 (m, 2H; $CH_{2(cod)}$), 1.78–1.70 (m, 2H; $CH_{2(cod)}$), 1.40 (d, $^3J=6.9$ Hz, 6H; $CH(CH_3)_2$), 1.21 (d, $^3J=6.9$ Hz, 6H; $CH(CH_3)_2$), 1.14 (d, $^3J=6.9$ Hz, 6H; $CH(CH_3)_2$), 1.13 ppm (d, $^3J=6.9$ Hz, 6H; $CH(CH_3)_2$); $^{13}C\{^1H\}$ NMR (125 MHz, CD_2Cl_2): $\delta=165.1$ (N=CH), 151.8 (N=CCH_3), 142.3 ($C_{(Ar)}$), 141.7 ($C_{(Ar)}$), 141.5 ($C_{(Ar)}$), 141.1 ($NCHN_{(near\ imine)}$), 140.8 ($C_{(Ar)}$), 139.0 ($C_{(Ar)}$), 136.6 ($C_{(Ar)}$), 129.1 ($CH_{(Ar)}$), 125.7 ($CH_{(Ar)}$), 124.1 ($CH_{(Ar)}$), 123.9 ($CH_{(Ar)}$), 71.1 ($CH_{(cod)}$), 70.3 ($CH_{(cod)}$), 31.6 ($CH_{2(cod)}$), 31.4 ($CH_{2(cod)}$), 28.8 ($CH(CH_3)_2$), 28.6 ($CH(CH_3)_2$), 25.9 ($CH(CH_3)_2$), 23.8 ($CH(CH_3)_2$), 22.8 ($CH(CH_3)_2$), 22.4 ($CH(CH_3)_2$), 18.1 ($CH_{3(imine)}$), 14.6 ppm ($CH_{3(imidazole)}$); $^{31}P\{^1H\}$ NMR (121.5 MHz, CD_2Cl_2): $\delta=-144.2$ ppm (sept, $^1J(P,F)=712$ Hz, PF_6^-); $^{19}F\{^1H\}$ NMR (282.4 MHz, CD_2Cl_2): $\delta=-73.3$ (d, $^1J(P,F)=712$ Hz, PF_6^-); IR (pure, orbit diamond): $\tilde{\nu}_{max}=1689$ (ν(C=N)), 1623 cm^{-1} (ν(C=N)); elemental analysis calcd for $C_{39}H_{54}F_6IrN_4P$ (916.07): C 51.13, H 5.94, N 6.12; found: C 50.56, H 5.96, N 5.88.

Synthesis of $[Ir_2(cod)_2Cl(L^{C2,Nimine,N3})]$ (10)

*From complex **1a**:* To a stirred yellow solution of complex **1a** (0.151 g, 0.25 mmol) in THF (10 mL) was added slowly a solution of KHMDS (0.55 g, 0.28 mmol) in THF (5 mL) at −78 °C. The reaction mixture was stirred for 1 h at −30 °C and the color of the solution turned to red. Then a solution of $[Ir(cod)(\mu\text{-}Cl)]_2$ (0.084 g, 0.13 mmol) in THF (5 mL) was added to the reaction mixture at −78 °C. The reaction mixture was further stirred for 12 h at room temperature during which time the color of the solution turned dark green. After removal of the solvent under reduced pressure, the residue was extracted with toluene and the solution was filtered through Celite. The filtrate was concentrated to approximately 3 mL. After Et_2O (3 mL) was added, the solution was cooled to −30 °C to yield dark green crystals, which were collected by filtration and dried in vacuo (0.145 g, 0.16 mmol, 64%). Single crystals of complex **10**·Et_2O·toluene suitable for X-ray diffraction were obtained by crystallization from a toluene/Et_2O (1:1) solution at −30 °C. ^1H NMR (400 MHz, C_6D_6): $\delta=7.29$ (d, $^3J=2.0$ Hz, 1H; NC*H*CHN$_{(near\ imine)}$), 7.07–6.86 (m, 3H; $CH_{(Dipp)}$), 6.30 (d, $^3J=2.0$ Hz, 1H; NCHC*H*N$_{(near\ imine)}$), 6.28–6.18 (m, 2H; $CH_{(cod)}$), 4.97–4.89 (m, 1H; $CH_{(cod)}$), 4.88–4.80 (m, 1H; $CH_{(cod)}$), 3.65–3.57 (m, 1H; $CH_{(cod)}$), 3.44–3.36 (m, 1H; $CH_{(cod)}$), 3.36–3.28 (m, 1H; $CH_{(cod)}$), 3.27–3.19 (m, 1H; $CH_{(cod)}$), 2.92 (sept, $^3J=6.7$ Hz, 2H; $CH(CH_3)_2$), 2.60–2.08 (m, 7H; $CH_{2(cod)}$), 2.06–1.76 (m, 3H; $CH_{2(cod)}$), 1.72–1.30 (m, 9H; $CH_{2(cod)}$, $CH_{3(imine)}$), 1.18 (d, $^3J=6.7$ Hz, 3H; $CH(CH_3)_2$), 1.11 (d, $^3J=6.7$ Hz, 3H; $CH(CH_3)_2$), 0.86 (d, $^3J=6.7$ Hz, 3H; $CH(CH_3)_2$), 0.54 ppm (d, $^3J=6.7$ Hz, 3H; $CH(CH_3)_2$). $^{13}C\{^1H\}$ NMR (75 MHz, C_6D_6): $\delta=180.6$ ($NCN_{(near\ imine)}$), 166.0 (C=N), 142.0 (*o*-$C_{(Dipp)}$), 141.8 (*o*-$C_{(Dipp)}$), 138.8 (*ipso*-$C_{(Dipp)}$), 131.8 ($NCHCHN_{(near\ imine)}$), 128.5 (*p*-$CH_{(Dipp)}$), 124.3 (*m*-$CH_{(Dipp)}$), 123.9 (*m*-$CH_{(Dipp)}$), 114.9 ($NCHCHN_{(near\ imine)}$), 83.1, 82.1, 70.8, 69.3, 68.1, 66.0, 59.0, 56.3 ($CH_{(cod)}$), 35.0, 33.8, 33.1, 32.6, 32.3, 31.6, 30.8, 29.4 ($CH_{2(cod)}$), 28.4, 28.0 ($CH(CH_3)_2$), 25.0, 24.7, 23.6, 23.0 ($CH(CH_3)_2$), 15.2 ppm ($CH_{3(imine)}$); IR (pure, orbit diamond): $\tilde{\nu}_{max}=1577$ (ν(C=N)), 292cm^{-1} (ν(Ir–Cl)); elemental analysis calcd for $C_{33}H_{46}ClIr_2N_3$ (904.64): C 43.81, H 5.13, N 4.65; found: C 43.38, H 4.85, N 4.21.

From complex $\mathbf{3a}^+[PF_6]^-$: To solution of complex $\mathbf{3a}^+[PF_6]^-$ (0.007 g, 0.010 mmol) in CD_2Cl_2 (0.5 mL) in a Young NMR tube, was added NaO*t*Bu (0.001 g, 0.010 mmol). The deprotonation was confirmed by ^1H NMR spectroscopic data after 30 min at room temperature.[19] Then $[Ir(cod)(\mu\text{-}Cl)]_2$ (0.004 g, 0.006 mmol) was added to the reaction mixture. The formation of complex **10** (>80%) was confirmed by ^1H NMR spectroscopic data after 30 min at room temperature.

Synthesis of $[Ir_2(CO)_4Cl(L^{C2,Nimine,N3})]$ (11): A solution of complex **10** (0.090 g, 0.10 mmol) in THF (2 mL) was stirred under CO (1 bar) at room temperature for 30 min and then filtered through a cannula. After removal of the volatiles under reduced pressure, the residue was washed with cold Et_2O (2×1 mL) to yield a red crystalline solid, which was collected by filtration and dried in vacuo (0.066 g, 0.082 mmol, 82%). Single crystals of complex **11** suitable for X-ray diffraction were obtained by slow diffusion of a layer of Et_2O into a solution of complex **11** in dichloromethane at ambient temperature under argon. ^1H NMR (500 MHz, CD_2Cl_2): $\delta=7.40$–7.30 (m, 3H; $CH_{(Dipp)}$), 7.22 (d, $^3J=2.1$ Hz, 1H; NCHC*H*N$_{(near\ imine)}$), 7.19 (d, $^3J=2.1$ Hz, 1H; NC*H*CHN$_{(near\ imine)}$), 3.09 (sept, $^3J=6.8$ Hz, 2H; $CH(CH_3)_2$), 2.34 (s, 1H; $CH_{3(imine)}$), 1.34 (d, $^3J=6.8$ Hz, 6H; $CH(CH_3)_2$), 1.18 ppm (d, $^3J=6.8$ Hz, 6H; $CH(CH_3)_2$); $^{13}C\{^1H\}$ NMR (125 MHz, CD_2Cl_2): $\delta=186.5$ ($NCN_{(near\ imine)}$), 183.0 (CO), 174.5 (CO), 172.3 (CO), 168.8 (C=N), 168.5 (CO), 142.7 (*ipso*-$C_{(Dipp)}$), 140.8 (*o*-$C_{(Dipp)}$), 133.0 ($NCHCHN_{(near\ imine)}$), 129.5 (*p*-$CH_{(Dipp)}$), 125.1 (*m*-$CH_{(Dipp)}$), 117.5 ($NCHCHN_{(near\ imine)}$), 28.9 ($CH(CH_3)_2$), 24.2 ($CH(CH_3)_2$), 23.7 ($CH(CH_3)_2$), 15.0 ppm ($CH_{3(imine)}$); IR (pure, orbit diamond): $\tilde{\nu}_{max}=2054$, 1971 (ν(CO)), 1606 (ν(C=N)), 320 cm^{-1} (ν(Ir–Cl)); elemental analysis calcd for $C_{21}H_{22}ClIr_2N_3O_4$ (800.30): C 31.52, H 2.77, N 5.25; found: C 32.06, H 3.23, N 5.32.

Synthesis of $[IrRh(cod)_2Cl(L^{C2,Nimine,N3})]$ (12)

*From complex **1b**:* To a stirred, yellow solution of complex **1b** (0.103 g, 0.20 mmol) in THF (10 mL) was added a solution of KHMDS (0.044 g, 0.22 mmol) in THF (5 mL) slowly at −78 °C. The mixture was stirred for 1 h at −30 °C and the color of the solution turned to orange. Then a solution of $[Ir(cod)(\mu\text{-}Cl)]_2$ (0.067 g, 0.10 mmol) in THF (5 mL) was added to the mixture at −78 °C. The mixture was further stirred for 12 h at room temperature during which time the color of the solution turned to maroon. After removal of the volatiles under reduced pressure, the residue was extracted with toluene and the solution was filtered through Celite. The filtrate was evaporated to dryness under reduced pressure. The residue was dissolved in THF (2 mL) and Et_2O (2 mL) was added. Then the solution was cooled to −30 °C to yield a maroon crystalline solid, which was collected by filtration and dried in vacuo (0.098 g, 0.12 mmol, 60%). Single crystals of complex **12**·2THF suitable for X-ray diffraction were obtained by crystallization in a THF/Et_2O (1:1) solution at −30 °C. ^1H NMR (500 MHz, CD_2Cl_2): $\delta=7.30$ (d, $^3J=1.8$ Hz, 1H; NC*H*CHN$_{(near\ imine)}$), 7.29–7.21 (m, 3H; $CH_{(Dipp)}$), 6.92 (d, $^3J=1.8$ Hz, 1H; NCHC*H*N$_{(near\ imine)}$), 6.26–6.18 (m, 1H; $CH_{(cod)}$), 5.57–5.49 (m, 1H; $CH_{(cod)}$), 4.57–4.49 (m, 1H; $CH_{(cod)}$), 4.46–4.38 (m, 1H; $CH_{(cod)}$), 3.66–3.54 (m, 2H; $CH_{(cod)}$), 3.52–3.40 (m, 1H; $CH_{(cod)}$), 3.32–3.22 (m, 1H; $CH_{(cod)}$), 3.21 (sept, $^3J=6.7$ Hz, 1H; $CH(CH_3)_2$), 3.07 (sept, $^3J=6.7$ Hz, 1H; $CH(CH_3)_2$), 2.70–

2.56 (m, 2H; $CH_{2(cod)}$), 2.44–2.28 (m, 4H; $CH_{2(cod)}$), 2.27–2.07 (m, 5H; $CH_{2(cod)}$, $CH_{3(imine)}$), 2.06–1.96 (m, 2H; $CH_{2(cod)}$), 1.95–1.85 (m, 2H; $CH_{2(cod)}$), 1.78–1.56 (m, 4H; $CH_{2(cod)}$), 1.35 (d, $^3J=6.7$ Hz, 3H; $CH(CH_3)_2$), 1.34 (d, $^3J=6.7$ Hz, 3H; $CH(CH_3)_2$), 1.12 (d, $^3J=6.7$ Hz, 3H; $CH(CH_3)_2$), 1.03 ppm (d, $^3J=6.7$ Hz, 3H; $CH(CH_3)_2$); $^{13}C\{^1H\}$ NMR (125 MHz, CD_2Cl_2): $\delta=179.8$ ($NCN_{(near\ imine)}$), 166.3 (C=N), 142.2 (*o*-$C_{(Dipp)}$), 142.0 (*o*-$C_{(Dipp)}$), 138.8 (*ipso*-$C_{(Dipp)}$), 131.7 ($NCHCHN_{(near\ imine)}$), 128.2 (*p*-$CH_{(Dipp)}$), 124.5 (*m*-$CH_{(Dipp)}$), 124.2 (*m*-$CH_{(Dipp)}$), 115.2 ($NCHCHN_{(near\ imine)}$), 84.8 (d, $^1J(Rh,C)=11.2$ Hz, $CH_{(cod)}$), 84.2 ($CH_{(cod)}$), 83.4 (d, $^1J(Rh,C)=11.4$ Hz, $CH_{(cod)}$), 83.0 ($CH_{(cod)}$), 77.9 (d, $^1J(Rh,C)=14.6$ Hz, $CH_{(cod)}$), 73.8 (d, $^1J(Rh,C)=13.8$ Hz, $CH_{(cod)}$), 69.2 ($CH_{(cod)}$), 65.4 ($CH_{(cod)}$), 34.5, 33.1, 32.8, 31.9, 31.3, 30.7, 29.5, 29.4 ($CH_{2(cod)}$), 28.6, 28.3 ($CH(CH_3)_2$), 25.3, 23.7, 23.4 ($CH(CH_3)_2$), 15.9 ppm ($CH_{3(imine)}$); IR (pure, orbit diamond): $\tilde{\nu}_{max}=1600$ (ν(C=N)), 290 cm^{-1} (ν(Rh–Cl)); elemental analysis calcd for $C_{33}H_{46}ClIrRhN_3$ (815.32): C 48.61, H 5.69, N 5.15; found: C 48.40, H 6.19, N 4.63.

From complex ***1a***: To a stirred solution of complex **1a** (0.121 g, 0.20 mmol) in THF (10 mL) was added slowly a solution of KHMDS (0044 g, 0.22 mmol) in THF (5 mL) at −78 °C. The reaction mixture was stirred for 1 h at −30 °C and the color of the solution turned to red. Then a solution of $[Rh(cod)(\mu\text{-}Cl)]_2$ (0.050 g, 0.10 mmol) in THF (5 mL) was added to the mixture at −78 °C. The reaction mixture was further stirred for 12 h at room temperature during which time the color of the solution turned maroon. After removal of the volatiles under reduced pressure, the residue was extracted with toluene and the solution was filtered through Celite. The filtrate was evaporated to dryness under reduced pressure. The residue was dissolved in THF (2 mL) and Et_2O (2 mL) was added. The solution was cooled to −30 °C to yield a maroon crystalline solid, which was collected by filtration and dried in vacuo (0.083 g, 0.10 mmol, 51%).

X-ray data collection, structure solution, and refinement for all compounds: Suitable crystals for the X-ray analysis of all compounds were obtained as described above. Data for complexes **1b**, **3b**$^+[PF_6]^-$, **7a**$^+[PF_6]^-$, **10**·Et_2O·toluene, and **12**·2THF were collected on an APEX-II CCD (graphite-monochromated $Mo_{K\alpha}$ radiation, $\lambda=0.71073$ Å) at 173(2) K, data for complexes **6a**$^+[PF_6]^-$, **9**$^+[PF_6]^-$, and **11** were collected on a Kappa CCD diffractometer (graphite-monochromated $Mo_{K\alpha}$ radiation, $\lambda=0.71073$ Å) at 173(2) K. Crystallographic and experimental details for these structures are summarized in Tables S1 and S2 in the Supporting Information. The structures were solved by direct methods (SHELXS-97[26]) and refined by full-matrix least-squares procedures (based on F^2, SHELXL-97[26]) with anisotropic thermal parameters for all the non-hydrogen atoms. The hydrogen atoms were introduced into the geometrically calculated positions (SHELXS-97 procedures). Details of the specific comments applied for the structures are provided in the Supporting Information. CCDC 1426156 (**1b**), 1426157 (**3b**$^+[PF_6]^-$), 1426158 (**6a**$^+[PF_6]^-$), 1426159 (**7a**$^+[PF_6]^-$), 1426160 (**9**$^+[PF_6]^-$), 1426161 (**10**·Et_2O·toluene), 1426162 (**11**), and 1426163 (**12**·2THF) contain the supplementary crystallographic data. These data can be obtained free of charge from The Cambridge Crystallographic Data Centre.

Acknowledgements

The USIAS, the CNRS, the UdS, the Région Alsace, and the Communauté Urbaine de Strasbourg are gratefully acknowledged for the award of fellowships and a Gutenberg Excellence Chair (2010-11) to A.A.D. and for support. We also thank the ucFRC (http://www.icfrc.fr) for support and the China Scholarship Council for a PhD grant to F.H., and the Service de Radiocristallographie (Institut de Chimie, Strasbourg) for the determination of the crystal structures.

Keywords: C–H activation · imidazoles · iridium · N-heterocyclic carbenes · rhodium

[1] a) A. J. Arduengo III, R. L. Harlow, M. Kline, *J. Am. Chem. Soc.* **1991**, *113*, 361–363; b) A. J. Arduengo III, H. V. R. Dias, R. L. Harlow, M. Kline, *J. Am. Chem. Soc.* **1992**, *114*, 5530–5534; c) D. Bourissou, O. Guerret, F. P. Gabbaï, G. Bertrand, *Chem. Rev.* **2000**, *100*, 39–92.

[2] a) F. E. Hahn, M. C. Jahnke, *Angew. Chem. Int. Ed.* **2008**, *47*, 3122–3172; *Angew. Chem.* **2008**, *120*, 3166–3216; b) P. de Frémont, N. Marion, S. P. Nolan, *Coord. Chem. Rev.* **2009**, *253*, 862–892; c) M. Melaimi, M. Soleilhavoup, G. Bertrand, *Angew. Chem. Int. Ed.* **2010**, *49*, 8810–8849; *Angew. Chem.* **2010**, *122*, 8992–9032; d) R. H. Crabtree, *Coord. Chem. Rev.* **2013**, *257*, 755–766.

[3] a) N. Meier, F. E. Hahn, T. Pape, C. Siering, S. R. Waldvogel, *Eur. J. Inorg. Chem.* **2007**, 1210–1214; b) F. E. Hahn, *ChemCatChem* **2013**, *5*, 419–430; c) M. C. Jahnke, F. E. Hahn, *Coord. Chem. Rev.* **2015**, *293–294*, 95–115.

[4] S. Karmakar, A. Datta, *Angew. Chem. Int. Ed.* **2014**, *53*, 9587–9591; *Angew. Chem.* **2014**, *126*, 9741–9745.

[5] F. E. Hahn in *Advances in Organometallic Chemistry and Catalysis* (Ed.: A. J. L. Pombeiro), Wiley, New York, **2013**, pp. 111–132.

[6] R. J. Sundberg, R. F. Bryan, I. F. Taylor, H. Taube, *J. Am. Chem. Soc.* **1974**, *96*, 381–392.

[7] a) R. Das, C. G. Daniliuc, F. E. Hahn, *Angew. Chem. Int. Ed.* **2014**, *53*, 1163–1166; *Angew. Chem.* **2014**, *126*, 1183–1187; b) R. Das, A. Hepp, C. G. Daniliuc, F. E. Hahn, *Organometallics* **2014**, *33*, 6975–6987.

[8] J. Tornatzky, A. Kannenberg, S. Blechert, *Dalton Trans.* **2012**, *41*, 8215–8225.

[9] a) K. L. Tan, R. G. Bergman, J. A. Ellman, *J. Am. Chem. Soc.* **2001**, *123*, 2685–2686; b) K. L. Tan, R. G. Bergman, J. A. Ellman, *J. Am. Chem. Soc.* **2002**, *124*, 3202–3203; c) K. L. Tan, A. Vasudevan, R. G. Bergman, J. A. Ellman, A. J. Souers, *Org. Lett.* **2003**, *5*, 2131–2134.

[10] a) K. L. Tan, R. G. Bergman, J. A. Ellman, *J. Am. Chem. Soc.* **2002**, *124*, 13964–13965; b) K. L. Tan, S. Park, J. A. Ellman, R. G. Bergman, *J. Org. Chem.* **2004**, *69*, 7329–7335; c) J. C. Lewis, R. G. Bergman, J. A. Ellman, *Acc. Chem. Res.* **2008**, *41*, 1013–1025.

[11] K. Araki, S. Kuwata, T. Ikariya, *Organometallics* **2008**, *27*, 2176–2178.

[12] a) V. Miranda-Soto, D. B. Grotjahn, A. G. DiPasquale, A. L. Rheingold, *J. Am. Chem. Soc.* **2008**, *130*, 13200–13201; b) V. Miranda-Soto, D. B. Grotjahn, A. L. Cooksy, J. A. Golen, C. E. Moore, A. L. Rheingold, *Angew. Chem. Int. Ed.* **2011**, *50*, 631–635; *Angew. Chem.* **2011**, *123*, 657–661.

[13] F. E. Hahn, A. R. Naziruddin, A. Hepp, T. Pape, *Organometallics* **2010**, *29*, 5283–5288.

[14] A. R. Naziruddin, A. Hepp, T. Pape, F. E. Hahn, *Organometallics* **2011**, *30*, 5859–5866.

[15] a) L. K. Johnson, C. M. Killian, M. Brookhart, *J. Am. Chem. Soc.* **1995**, *117*, 6414–6415; b) B. L. Small, M. Brookhart, A. M. A. Bennett, *J. Am. Chem. Soc.* **1998**, *120*, 4049–4050; c) G. J. P. Britovsek, V. C. Gibson, S. J. McTavish, G. A. Solan, A. J. P. White, D. J. Williams, G. J. P. Britovsek, B. S. Kimberley, P. J. Maddox, *Chem. Commun.* **1998**, 849–850; d) C. C. H. Atienza, T. Diao, K. J. Weller, S. A. Nye, K. M. Lewis, J. G. P. Delis, J. L. Boyer, A. K. Roy, P. J. Chirik, *J. Am. Chem. Soc.* **2014**, *136*, 12108–12118.

[16] a) K. S. Coleman, S. Dastgir, G. Barnett, M. J. P. Alvite, A. R. Cowley, M. L. H. Green, *J. Organomet. Chem.* **2005**, *690*, 5591–5596; b) M. Frøseth, K. A. Netland, C. Rømming, M. Tilset, *J. Organomet. Chem.* **2005**, *690*, 6125–6132; c) S. Dastgir, K. S. Coleman, A. R. Cowley, M. L. H. Green, *Organometallics* **2006**, *25*, 300–306; d) J. Al Thagfi, S. Dastgir, A. J. Lough, G. G. Lavoie, *Organometallics* **2010**, *29*, 3133–3138; e) J. Al Thagfi, G. G. Lavoie, *Organometallics* **2012**, *31*, 2463–2469; f) P. Liu, M. Wesolek, A. A. Danopoulos, P. Braunstein, *Organometallics* **2013**, *32*, 6286–6297.

[17] a) M. L. Rosenberg, A. Krivokapic, M. Tilset, *Org. Lett.* **2009**, *11*, 547–550; b) M. L. Rosenberg, K. Vlašaná, N. S. Gupta, D. Wragg, M. Tilset, *J. Org. Chem.* **2011**, *76*, 2465–2470.

[18] a) S. Kuwata, T. Ikariya, *Chem. Eur. J.* **2011**, *17*, 3542 – 3556; b) S. Kuwata, T. Ikariya, *Chem. Commun.* **2014**, *50*, 14290 – 14300; c) B. Zhao, Z. Han, K. Ding, *Angew. Chem. Int. Ed.* **2013**, *52*, 4744 – 4788; *Angew. Chem.* **2013**, *125*, 4844 – 4889.

[19] F. He, P. Braunstein, M. Wesolek, A. A. Danopoulos, *Chem. Commun.* **2015**, *51*, 2814 – 2817.

[20] F. He, L. Ruhlmann, J.-P. Gisselbrecht, S. Choua, M. Orio, M. Wesolek, A. Danopoulos, P. Braunstein, *Dalton Trans.* **2015**, *44*, 17030 – 17044.

[21] T. Kösterke, J. Kösters, E.-U. Würthwein, C. Mück-Lichtenfeld, C. Schulte to Brinke, F. Lahoz, F. E. Hahn, *Chem. Eur. J.* **2012**, *18*, 14594 – 14598.

[22] a) C. Bianchini, E. Farnetti, M. Graziani, G. Nardin, A. Vacca, F. Zanobini, *J. Am. Chem. Soc.* **1990**, *112*, 9190 – 9197; b) M. T. Whited, R. H. Grubbs, *Organometallics* **2008**, *27*, 5737 – 5740; c) G. Song, Y. Su, R. A. Periana, R. H. Crabtree, K. Han, H. Zhang, X. Li, *Angew. Chem. Int. Ed.* **2010**, *49*, 912 – 917; *Angew. Chem.* **2010**, *122*, 924 – 929.

[23] G. E. Dobereiner, C. A. Chamberlin, N. D. Schley, R. H. Crabtree, *Organometallics* **2010**, *29*, 5728 – 5731.

[24] G. Giordano, R. H. Crabtree, R. M. Heintz, D. Forster, D. E. Morris in, *Inorganic Syntheses, Vol. 28* (Ed.: R. J. Angelici), Wiley, Hoboken, **1990**, pp. 88 – 90.

[25] H. Graboyes, T. J. Kasper, P. D. Vaidya, Eur. Pat. Appl., **1982**, EP49638.

[26] SHELXL-97, Program for crystal structure refinement, G. M. Sheldrick, University of Göttingen, Göttingen (Germany), **1997**.

Received: October 8, 2015
Published online on January 15, 2016